JOINT INVERSION OF PRODUCTION AND TEMPERATURE DATA ILLUMINATES VERTICAL PERMEABILITY DISTRIBUTION IN DEEP RESERVOIRS

A Thesis

by

ZHISHUAI ZHANG

Submitted to the Office of Graduate Studies of
Texas A&M University
in partial fulfillment of the requirements for the degree of

MASTER OF SCIENCE

August 2012

Major Subject: Petroleum Engineering

Joint Inversion of Production and Temperature Data Illuminates Vertical Permeability Distribution in Deep Reservoirs

JOINT INVERSION OF PRODUCTION AND TEMPERATURE DATA ILLUMINATES VERTICAL PERMEABILITY DISTRIBUTION IN DEEP RESERVOIRS

A Thesis

by

ZHISHUAI ZHANG

Submitted to the Office of Graduate Studies of
Texas A&M University
in partial fulfillment of the requirements for the degree of

MASTER OF SCIENCE

Approved by:

Co-Chairs of Committee,	Behnam Jafarpour
	Akhil Datta-Gupta
Committee Members,	Michael King
	Wolfgang Bangerth
Head of Department,	Dan Hill

August 2012

Major Subject: Petroleum Engineering

ABSTRACT

Joint Inversion of Production and Temperature Data Illuminates Vertical Permeability Distribution in Deep Reservoirs. (August 2012)

Zhishuai Zhang, B.S., Nankai University

Co-Chairs of Advisory Committee: Dr. Behnam Jafarpour
Dr. Akhil Datta-Gupta

Characterization of connectivity in compartmentalized deepwater Gulf of Mexico (GoM) reservoirs is an outstanding challenge of the industry that can significantly impact the development planning and recovery from these assets. In these deep formations, temperature gradient can be quite significant and temperature data can provide valuable information about field connectivity, vertical fluid displacement, and permeability distribution in the vertical direction. In this paper, we examine the importance of temperature data by integrating production and temperature data jointly and individually and conclude that including the temperature data in history matching of deep GoM reservoirs can increase the resolution of reservoir permeability distribution map in the vertical direction.

To illustrate the importance of temperature measurements, we use a coupled heat and fluid flow transport model to predict the heat and fluid transport in the reservoir. Using this model we ran a series of data integration studies including: 1) integration of production data alone, 2) integration of temperature data alone, and 3) joint integration of production and temperature data. For data integration, we applied four algorithms:

Maximum A-Posteriori (MAP), Randomized Maximum Likelihood (RML), Sparsity Regularized Reconstruction and Sparsity Regularized RML methods. The RML and Sparsity Regularized RML approaches were used because they allow for uncertainty quantification and estimation of reservoir heterogeneity at a higher resolution. We also investigated the sensitivity of temperature and production data to the distribution of permeability, which showed that while production data primarily resolved the distribution of permeability in the horizontal direction, the temperature data did not display much sensitivity to permeability in the horizontal extent of the reservoir. The results of these experiments were compelling in that they clearly illuminated the role of temperature data in enhancing the resolution of reservoir permeability maps with depth. We present several experiments that clearly illustrate and support the conclusions of this study.

DEDICATION

To my parents and grandparents for their love

ACKNOWLEDGEMENTS

I would like to express my sincere gratitude to Dr. Behnam Jafarpour for providing me a great research environment and support. I really appreciate his patient guidance, invaluable advice, and kindly encourage in our weekly individual meeting and emails. None of this work would have been possible without him.

I gratefully thank my committee co-chair Dr. Akhil Datta-Gupta, committee members Dr. Michael King and Dr. Wolfgang Bangerth for their help and support in my research. I also thank Dr. Eduardo Gildin and Dr. George Moridis for their advice and suggestions. I would like to give special thanks to Dr. Lianlin Li who gives me a lot of advice and strong support on my research. Also, many thanks to group members Mohammad-Reza M. Khaninezhad, Mohammadali Tarrahi, Pongsathorn Lerelertpakee and Morteza Khodabakhshi for their help and friendship.

Thanks also go to all my friends and colleagues and the department faculty and staff for making my time at Texas A&M University a great experience.

Last, but not least, I would like to thank to my parents for their love and encouragement.

NOMENCLATURE

α	K-SVD coefficients
β	Compressibility
β_f	Fluid compressibility
β_s	Solid compressibility
C_M	Covariance matrix of model parameters
C_D	Covariance matrix of model observations
c_P	Constant pressure heat capacity
c_{Pf}	Fluid constant pressure heat capacity
c_{Ps}	Solid constant pressure heat capacity
$\mathbf{D}$	K-SVD trained dictionary
$\mathbf{d_{obs}}$	Observation data
e	Specific internal heat of heat of fluid
e_s	Specific internal heat of heat of fluid at source conditions
$\mathbf{f}$	State functions
G	Sensitivity matrix
$\mathbf{g}$	Model functions
γ	Variogram
h	Specific enthalpy
K	Number of dictionary elements
k	Thermal conductivity

k_f	Fluid thermal conductivity
k_s	Solid thermal conductivity
λ	Ajoint parameters
$\mathbf{m_{prior}}$	Prior model parameters
$\mathbf{m_{MAP}}$	Posterior model parameters using MAP estimation
μ	Viscosity
N	Number of ensemble realizations
P	Pressure
Φ	Sparse transformation matrix
φ	Porosity
$\tilde{q}$	Sources and sinks
ρ	Density
ρ_0	Density at standard condition
ρ_S	Density at source conditions
S	Number of non-zero elements
σ_m	Standard deviation of model parameter
σ_d	Standard deviation of observation
T	Temperature
T_S	Temperature of sources
t	Time
U	Internal energy
V	Volume

$\vec{v}$	Velocity
W	Diagonal Weighting Matrix

TABLE OF CONTENTS

Page

LIST OF FIGURES

LIST OF TABLES

CHAPTER I

INTRODUCTION AND LITERATURE REVIEW

Numerical reservoir simulations are widely used to predict the fluid flow and production behavior in subsurface environment. These simulations require knowledge of the property of porous media to determine the fluid behavior in the reservoir. The accuracy of the knowledge on porous media decides the confidence on the prediction of fluid flow and production behavior. One important property of rock is its permeability which is a measure of the ability of porous medium to transport fluid. Since the direct measurement of permeability at every point of the reservoir is costly and impossible, the spatial distribution of permeability is usually determined by integrating dynamic production data into prior knowledge of the reservoir, this process is called reservoir characterization, or history matching. Because of the limited number of observations comparing to the number of unknowns, the inverse problem is ill-posed. That is, more than one set of parameters are able to explain the observations equally well but only one set of them is true and can be used to predict the future behavior of the reservoir. There are two ways to solve the problem of ill-posedness and improve the accuracy of the solution. One is to seek for new observations and another is to add prior information on the reservoir to the inverse problem.

This thesis follows the style of *SPE Journal*.

In traditional history matching, it is common to use production rate and saturation of produced fluid to estimate the reservoir properties. However, because of the sparsity of available observations (Carrera and Neuman 1986; Carrera and Neuman 1986; Carrera and Neuman 1986), it is hard to determine the reservoir property accurately, especially in the case of estimation of heterogeneous distribution of permeability where the amount of unknown parameters is very large. In deepwater reservoir or geothermal reservoir, like deepwater Gulf of Mexico reservoirs (Hutchinson et al. 2007; Arnold et al. 2010), because of the geothermal gradient, temperature change with depth is significant. Due to this change in temperature, the fluid produced from the upper layer of the reservoir has a lower temperature while that produced from the lower layer of the reservoir has a higher temperature. Thus, production temperature carries information about hydraulic properties distribution with depth in the reservoir. In addition, the usage of modern monitor technology like permanent downhole distributed fiber optic sensors makes the accurate measurement of temperature of produced fluid possible (Brown et al. 2005; Fryer et al. 2005; Nath et al. 2006). The fiber optic sensor can be used in both oil gas reservoir and geothermal reservoir (Kragas et al. 2001; Ikeda Naotsugu 2002). So the integration of temperature into reservoir characterization is a promising method to improve the result of estimation. The inversions problem based on measurement of fiber optic sensor have been extensively studies (Yoshioka et al. 2009; Li and Zhu 2010). Li and Zhu (2010) presented a methodology for using downhole temperature measurement to improve the results of reservoir characterization. They used

a thermal model to estimate wellbore temperature distribution that gave large scale permeability trends.

The process of coupled fluid and heat flow in subsurface porous medium has been extensively studied for many years. A couple of commercial software for numerical simulation of coupled fluid and heat flow in subsurface have been developed (Pruess et al. 1999). The characterization of non-isothermal reservoir model from various observations has been investigated with Maximum A Posteriori estimation, Monte Carlo approach, and Ensemble Kalman Filter (Rath et al. 2006; Kiryukhin et al. 2008; Kühn and Gessner 2009; Mukhopadhyay 2009; Kosack et al. 2010). However, how much and why the temperature observation contributes to the characterization are unknown.

Adding prior knowledge on the reservoir properties is another way to improve the accuracy and reliability of the history matching results. The prior knowledge is usually incorporated as a regularization term into the objective function to regularize the inverse problem. The prior knowledge is usually about the structural properties of the reservoir, that is, enforce the solution to be spatially smoothed according to certain assumption on the spatial correlations between two points.

One way to incorporate the regularized term is to assume the reservoir is uniform before the process of integration of dynamic data, and use the covariance between each pair of grid point calculated from a certain variogram model to form a covariance matrix to enforce the smoothness of the reservoir. This results in a commonly used reservoir characterization method known as Maximum A-Posteriori (MAP) method (Tarantola

and Valette 1982; Tarantola and Valette 1982; Oliver et al. 2008). However, the MAP estimation is based on the assumption of the Gaussian distribution and the linearity of the model. In practical application, the posterior variance given by the MAP estimation is unreasonable. To access the uncertainty of the posterior estimation result, we can generate multiple samples from a posterior probability density function. One way to generate realizations is Randomized Maximum Likelihood (RML) estimation(Oliver et al. 1996; Feng et al. 2009). RML is an approximation of Markov chain Monte Carlo so that it can sample from the posterior distribution even the problem is nonlinear and non-Gaussian.

In both MAP estimation and RML estimation, we need the gradient of the objective function with respect to the unknown parameter to minimize the objective function. Because of the nonlinearity and complexity of subsurface process, it is difficult to evaluate the gradient of the objective function with respect to the permeability of heterogeneous reservoir. The traditional finite numerical methods like finite difference method require a huge amount of computation time for problem with many parameters to be estimated. To make things worse, the truncation error makes it may take several trials to choose a reasonable perturbation amount. One alternative is automatic differention (AD) technique. The principle idea behind AD is that every computer program executes a sequence of elementary arithmetic operations and elementary functions whose derivatives are known, so by applying the chain rule repeatedly to these operator and functions, the derivative can be obtained without truncation error. Tools for implementing AD are available for various programming languages like C++, C

(Griewank et al. 1996; Bischof et al. 1997), Fortran (Bischof et al. 1996; Giering and Kaminski 1998), and MATLAB (Bischof et al. 2002). The application of AD in subsurface inversion was done by Rath et al. (2006). A more efficient way to calculate the gradient is the adjoint method. The adjoint method is a method of evaluating the gradient by adjoining the constraint to the objective function (Neuman and Carrera 1985; Marchuk 1995; Marchuk et al. 1996; Bunge et al. 2003; Oliver et al. 2008). It is a very computational efficient method and with the implementation of adjoint method in the simulation code, one can do the characterization of heterogeneous reservoir with gradient based method in a very efficient way. Because of the difficulty of its implementation, the adjoint method is not widely used in research especially in joint inversion of production rate and temperature observations which leave a lot of interesting thing remained to be done.

Another way to incorporate the regularization is to enforce the solution to be sparse in certain sparse transformation domain (Khaninezhad et al. 2010; Li and Jafarpour 2010). Li and Jafapour (2010) proposed an iteratively reweighted least-squares inversion algorithm to incorporate the sparsity of the reservoir properties under DCT and DWT transformation. Then, Khaninezhad et al. (2010) applied this method to a geologically motivated sparse bases constructed by K-SVD which make the characterization of the reservoir more specialized and accurate. Both of these two works are demonstrated using an isothermal two dimensional reservoir model and the effectiveness of these methods under three dimensional non-isothermal reservoir models remains to be tested.

In the remaining part of this paper is organized as follows. In chapter II, the principles and methodologies for the characterization of non-isothermal reservoir will be introduced including basic governing equations for forward model, estimation methods used in the reservoir characterization, adjoint method for gradient calculation, etc. In chapter III, the model and experiment setup will be presented and followed with the MAP, RML, K-SVD methods characterization results. In addition, a comparison on characterization results from various observations will be made. Chapter IV will conclude and summarize the paper.

CHAPTER II

THEORY AND METHODOLOGY

2.1 Non-isothermal Reservoir Model

Coupled fluid and heat flow in porous medium has been studied for many years, and a comprehensive model is presented by Bejan (Bejan 2004). According to Bejan, this process can be decided by a combination of mass conservation equation, energy conservation equation and darcy's law.

2.1.1 Mass conservation equation

$$D\rho/Dt + \rho\nabla\cdot\vec{v} = \rho_0\tilde{q} \tag{2.1}$$

where ρ is the density of fluid in reservoir condition while ρ_0 is the density of fluid at standard condition. $\vec{v} = u\hat{\imath} + v\hat{\jmath} + w\hat{k}$ is the velocity of fluid. $\tilde{q}$ is the volume of injected (+) or produced fluid (-) at standard condition in unit reservoir volume and unit time. D/Dt is material derivative defined as $\partial/\partial t + u\times\partial/\partial x + v\times\partial/\partial y + w\times\partial/\partial z$.

2.1.2 Energy conservation equation

Using a similar approach with Bejan (Bejan 2004; Duru 2008), we can derive the energy conservation equation with sources and sinks as the Eq.2.

$$\rho\times De/Dt + e\rho_0\tilde{q} = \nabla\cdot(k\nabla T) + e_s\rho_0\tilde{q} + P\tilde{q}\rho_0/\rho_s - P\nabla\cdot\vec{v} + \mu\Phi \tag{2.2}$$

where, P are the temperature and pressure of fluid. k , μ are thermal conductivity and viscosity of fluid. Φ is a function of the spatial derivative of velocity. In two dimension, $\Phi = 2[(\partial u/\partial x)^2 + (\partial u/\partial y)^2] + (\partial v/\partial y + \partial u/\partial x)^2$. e is specific internal

heat of fluid at reservoir condition. e_s is specific internal heat of fluid at sources and sinks condition (sources or sinks temperature, pressure at the sources and sinks position).

For a system of mass m, the internal energy change can be denoted as

$$\Delta U = (\Delta e)m = (e_s - e)m = -P\Delta V + c_p(T_s - T)m$$
$$= -P(\mathrm{m}/\rho_s - \mathrm{m}/\rho) + c_p(T_s - T)m \quad (2.3)$$

where ΔU, Δe and ΔV are the changes in internal energy, specific internal heat and volume of the fluid. T_s and T are temperature of fluid goes into and out of the system respectively. c_p is the constant pressure heat capacity of liquid. From Eq. 3, we can get

$$e_s - e = -P/\rho_s + P/\rho + c_p(T_s - T) \quad (2.4)$$

So the energy conservation equation becomes

$$\rho \times De/Dt = \nabla \cdot (k\nabla T) + \rho_0 \tilde{q} P/\rho + \rho_0 \tilde{q} c_p(T_s - T) - P\nabla \cdot \tilde{v} + \mu\Phi \quad (2.5)$$

To express the equation in terms of enthalpy, we use the thermodynamics definition of specific enthalpy

$$h = e + P/\rho \quad (2.6)$$

Apply the material derivative, we get

$$Dh/Dt = De/Dt + \rho \times DP/Dt - P/\rho^2 \times D\rho/Dt \quad (2.7)$$

Substitute the De/Dt with the Eq. 7. we get

$$\rho \times Dh/Dt = \nabla \cdot (k\nabla T) + \rho_0 \tilde{q} c_p(T_s - T) + DP/Dt + \mu\Phi \quad (2.8)$$

From thermodynamics, we can get

$$dh = c_p dT + (1 - \beta T) \times dP/\rho \quad (2.9)$$

where β is the coefficient of thermal expansion. For incompressible fluid, $\beta = 0$. For ideal gas, $\beta T = 1$.

The temperature formulation of the energy conservation equation is therefore

$$\rho c_p \times DT/Dt = \nabla \cdot (k\nabla T) + \rho_0 \tilde{q} c_p (T_s - T) + \beta T \times DP/Dt + \mu\Phi \qquad (2.10)$$

2.1.3 Darcy's Law

$$\vec{v} = -K\nabla P/\mu \qquad (2.11)$$

2.1.4 Energy conservation equation for porous medium

We start with the energy conservation equation for solid and fluid parts and average these equations to get the energy equation for porous medium.

For the solid part we have,

$$\rho_s c_{ps} \times DT/Dt = \nabla \cdot (k_s \nabla T) + \beta_s T \times DP/Dt \qquad (2.12)$$

To make things simpler, we make the assumption that the solid is incompressible so $\beta_s T \times DP/Dt = 0$.

For the fluid part we have,

$$\rho_f c_{pf} \times DT/Dt = \nabla \cdot \left(k_f \nabla T\right) + \rho_{f0} \tilde{q} c_{pf} (T_s - T) + \beta_f T \times DP/Dt + \mu\Phi \quad (2.13)$$

Combine energy equations for solid and fluid and then apply Darcy's Law, we get

$$\rho_f c_{pf} (\sigma \times \partial T/\partial t + \vec{v} \cdot \nabla T)$$

$$= \nabla \cdot (k\nabla T) + \rho_{f0} \tilde{q} c_{pf} (T_s - T) + \beta_f T\Phi \times \partial P/\partial t + \beta_f T\vec{v} \cdot \nabla P + \mu(\vec{v})^2/K \quad (2.14)$$

where $\sigma = \left(\Phi\rho_f c_{pf} + \left(1 - \Phi\rho_s c_{ps}\right)\right)/\rho_f c_{pf}$. The overall thermal conductivity $k = \Phi k_f + (1 - \Phi)k_s$.

The left hand side of the equation stands for the temperature change over time and the result of heat advection. $\nabla \cdot (k\nabla T)$ stands for the effect of thermal conduction and $\rho_{f0}\tilde{q}c_{pf}(T_s - T)$ is the sources and sinks term. $\beta_f T\Phi \times \partial P/\partial t + \beta_f T\vec{v} \cdot \nabla P$ is a result of thermal expansion and compression. And the last term is viscosity dissipation term.

But please notice this is valid only for One Dimensional problem in real applications (Bejan 2004); in general, the overall local thermal conductivity k can be decided by an extension of the model of Somerton (Somerton et al. 1973; Somerton et al. 1974; Moridis et al. 2005) or measured experimentally.

2.2 The Maximum A Posteriori (MAP) Estimation Method

The Bayesian framework allows one to combine observed production data and prior information on reservoir to obtain the a posteriori probability density function (PDF) of reservoir properties (Oliver et al. 2008; Zhang et al. 2003). Let $f(\mathbf{m}|\mathbf{d_{obs}})$ denote the posterior conditional PDF for model m given the observed N_d dimensional vector of data $\mathbf{d_{obs}}$and prior PDF for model $\mathbf{m_{prior}}$. Under the assumption that the prior PDF for the model m is Gaussian and that measurement and modeling errors are Gaussian, the posterior PDF can be obtained from the Bayes' theorem,

$$f(\mathbf{m}|\mathbf{d_{obs}}) =$$

$$a \exp\left[-(\mathbf{m} - \mathbf{m_{prior}})^T C_M^{-1}(\mathbf{m} - \mathbf{m}_{prior})/2 - (\mathbf{g}(\mathbf{m}) - \mathbf{d_{obs}})^T C_D^{-1}(\mathbf{g}(\mathbf{m}) - \mathbf{d_{obs}})/2\right] \quad (2.15)$$

where $m$is an $N_m$dimensional column vector, a is the normalizing constant, C_M is the $N_m \times N_m$ prior covariance matrix for the random vector m, C_D is the $N_d \times N_d$

covariance matrix for data measurement errors and modeling errors, $\mathbf{g}(\mathbf{m})$ is the assumed theoretical model for predicting data for a given $\mathbf{m}$, $\mathbf{d_{obs}}$ is the an $N_d$dimensional column vector containing measured conditioning data, and $\mathbf{m_{prior}}$ is the prior mean of the N_m dimensional column vector m.

However, because of the nonlinearity of the model, calculating the Eq. 14. is not easy even under the Gaussian assumption of the model. One method is to find the maximum a posteriori estimate of the model. The MAP estimate of the model which is denoted by m_{MAP} is the model that maximizes $f(\mathbf{m})$ or equivalently minimizes an objective function

$$O(\mathbf{m}) = \left(\mathbf{m} - \mathbf{m_{prior}}\right)^T C_M^{-1}\left(\mathbf{m} - \mathbf{m_{prior}}\right)/2 + (\mathbf{g}(\mathbf{m}) - \mathbf{d_{obs}})^T C_D^{-1}(\mathbf{g}(\mathbf{m}) - \mathbf{d_{obs}})/2 \tag{2.16}$$

i.e.

$$\mathbf{m_{MAP}} = \text{argmin}_m\, O(\mathbf{m}) \tag{2.17}$$

The minimization can be done with the classical Newton approach. Take the derivative of the objective function with respect to m, take the transpose and then rearrange, the above minimization problem can be solved through the following iteration.

$$\mathbf{m}^{n+1} = \left[\left(C_M^{-1} + C_M^{-1^T}\right) + G^{n^T}\left(C_D^{-1} + C_D^{-1^T}\right)G^n\right]$$
$$\backslash\left[\left(C_M^{-1} + C_M^{-1^T}\right)\mathbf{m_{prior}} + G^{n^T}\left(C_D^{-1} + C_D^{-1^T}\right)(\mathbf{d_{obs}} - \mathbf{g}(\mathbf{m}^n) + G^n\mathbf{m}^n)\right] \tag{2.18}$$

G is the sensitivity which is variation of $g(m)$ as a result of a small change in m

$$G = \begin{bmatrix} \partial g_1/\partial m_1 & \partial g_1/\partial m_2 & \cdots & \partial g_1/\partial m_n \\ \partial g_2/\partial m_1 & \partial g_2/\partial m_2 & \cdots & \partial g_2/\partial m_n \\ \vdots & \vdots & \ddots & \vdots \\ \partial g_m/\partial m_1 & \partial g_m/\partial m_2 & \cdots & \partial g_m/\partial m_n \end{bmatrix} \tag{2.19}$$

Once the most probable model $\mathbf{m_{MAP}}$ is obtained, the a poster covariance matrix $C_m{}'$ can be approximated based on linearization about the MAP estimate point by

$$C_{M,MAP} = (G_{MAP}^T C_D^{-1} G_{MAP} + C_M^{-1})^{-1} \tag{2.20}$$

2.3 Sensitivity Analysis and Adjoint Method

Sensitivity analysis is a way to measure the contribution of observed data to the estimation of the reservoir properties. The sensitivity G is the change of observation data because of a small perturbation on a reservoir property to be estimated. A higher value of the sensitivity coefficient means the observation is more sensitive to the corresponding reservoir property. Thus, it will result in a more accurate estimation of the corresponding parameter (Finsterle 1999).

However, because of the variation in unit and accuracy of observation and reservoir parameters, it is meaningless to compare the absolute value of sensitivity with each other. In order to make sensitivity coefficients comparable with one another, we can scale them by the standard deviation of the observation, σ_d, and the posterior parameter standard deviation, σ_m (Finsterle 1999).

$$\tilde{G}_{ij} = G_{ij} \times \sigma_m/\sigma_d \tag{2.21}$$

With the scaled sensitivity coefficients, we can compare the contribution of various observed data to the characterization of reservoir model. In addition, we can make the

summation of certain group of sensitivity coefficient to form composite sensitivity as a representation of the contribution of certain group of observations or the contribution to certain group of parameters.

One composite is the summation of the absolute values of the elements in a certain row of the scaled Jacobian matrix:

$$a_i = \sum_{j=1}^{n} \left| \tilde{G}_{ij} \right| \tag{2.22}$$

This composite sensitivity a_i is a measure of the contribution of observation i to the characterization of the whole reservoir model.

By making the summation of all the coefficients belonging to a certain group of observed data, the total contribution of these observations to the estimation of one unknown parameter j can be evaluated as the following composite sensitivity:

$$b_{kj} = \sum_{i=1}^{m} \left| \tilde{G}_{ij} \right|_{i \in k} \tag{2.23}$$

Reservoir estimation based on optimization method and sensitivity analysis requires knowledge of the gradient of the objective function with respect to the parameter at each point G_{ij}. For linear problem, sensitivity can be obtained easily. However, for realistic nonlinear flow and transport problems, the sensitivity need to be calculated by small perturbation on parameter or derived from the partial differential equations that govern flow and transport. The former method is straight forward but too computationally demanding to use in the characterization of subsurface heterogeneity. To make things worse, the determination of the perturbation amount may need several trials. Oliver presented the application of adjoint method in subsurface inversion which can be very efficient in deriving the sensitivity coefficients (Oliver et al. 2008).

Suppose we wish to compute the derivative of the following function with respect to model parameter **m.**

$$\mathbf{g} = \mathbf{g}\big(\mathbf{x}(\mathbf{m})\big) \tag{2.24}$$

subject to

$$\mathbf{f}^n(\mathbf{x}^{n+1}, \mathbf{x}^n, \mathbf{m}) = 0 \tag{2.25}$$

where $\mathbf{x}(\mathbf{m})$ are the reservoir states.

According to Oliver, we can obtain an adjoint function J by adjoining the constraint equations to the function **g**

$$J = \mathbf{g} + \sum_{n=0}^{L} (\lambda^{n+1})^T \mathbf{f}^{n+1} \tag{2.26}$$

where $\lambda^{n+1} = \left[\, \lambda_1^{n+1}, \lambda_2^{n+1}, \ldots, \lambda_{N_e}^{n+1} \right]^T$

Take the total differential and rearranging the above equation, the derivative can be obtained by the following

$$\frac{dJ}{d\mathbf{m}} = \nabla_{\mathbf{m}}\mathbf{g} + \sum_{n=1}^{L} [\nabla_{\mathbf{m}}(\mathbf{f}^n)^T](\lambda^n) \tag{2.27}$$

$$\lambda^{L+1} = 0 \tag{2.28}$$

$$[\nabla_{\mathbf{x}^n}(\mathbf{f}^n)^T]\lambda^n = -[\nabla_{\mathbf{x}^n}(\mathbf{f}^{n+1})^T]\lambda^{n+1} - \nabla_{\mathbf{x}^n}\mathbf{g} \tag{2.29}$$

2.4 Randomized Maximum Likelihood (RML) Method

The maximum a posteriori (MAP) estimation method is based on the assumption of Gaussian distribution of modeling and measurement errors and the linearity of the model. However, the linearity of subsurface fluid and heat flow model is not generally the case. For nonlinear case, the posteriori PDF is not necessarily Gaussian even though

the modeling and measurement errors are both Gaussian. To find multiple realizations from the a posteriori PDF to allow for local uncertainty analysis, we use the Randomized Maximum Likelihood calibrated realizations as trial states in a Markov chain Monte Carlo (McMC) method. The calculation of acceptance criterion is complex and we make an assumption to simply accept all the states that are the results of the calibration procedure. This assumption is demonstrated to be proper for a simple but highly nonlinear problem (Oliver et al. 1996).

Under this assumption, the RML method can be done in the following three procedures,

1. Generate an unconditional realization of the model variable $m_{u,i}$.
2. Generate an unconditional realization of the noise in the data and add the noise to the data to create $d_{u,i}$.
3. Compute the model $m_{c,i}$ that minimizes

$$S(m) = \left(m - m_{u,i}\right)^T C_M^{-1}\left(m - m_{u,i}\right) + \left(g(m) - d_{u,i}\right)^T C_D^{-1}\left(g(m) - d_{u,i}\right) \quad (2.30)$$

Repeat the above procedures for N times.

2.5 Variogram, Ordinary Kriging and Sequential Gaussian Simulation

2.5.1 Variogram

Variogram is a measure of dissimilarity between two random variables, traditionally has been used to model spatial variability

$$\gamma(\vec{L}) = var\left(X(u) - X\left(u + \vec{L}\right)\right)/2$$

$$= E\left[\left(X(u) - X\left(u + \vec{L}\right)\right)^2\right]/2 - E\left[\left(X(u) - X\left(u + \vec{L}\right)\right)\right]^2/2 \qquad (2.31)$$

The covariance matrix of the prior permeability and conductivity distribution can be generated based on information on variogram model. If the variogram model $\gamma(L)$ of the reservoir is known, the elements of the covariance matrix can be obtained according to

$$C(0) = \lim_{L\to\infty} \gamma(L) \qquad (2.32)$$

$$C(L) = C(0) - \gamma(L) \qquad (2.33)$$

$C(L)$ is auto-covariance which denotes the covariance between a random variable and its (time) space shifted version. Thus, $C(0)$ is the variance of a certain data point.

2.5.2 Ordinary Kriging

Let $\varphi(\mu)$ be a function of position. In kriging, we want to find a solution that honors data and spatial relationship between data and unknown as well as within data points (through variogram).

$$\phi^*(\mu_0) = \lambda_0 + \sum_{i=1}^{n} \lambda_i \phi(\mu_i) \qquad (2.34)$$

The desirable estimator properties are unbiasedness and minimum estimation error variance. In ordinary kriging, the stationary mean of the random field is unknown. Under these assumptions, the kriging weights can be obtained by

$$\lambda_0 = 0 \qquad (2.35)$$

$$\begin{bmatrix} C_{11} & C_{12} & C_{13} & \cdots & C_{1n} & 1 \\ C_{21} & C_{22} & C_{23} & & & 1 \\ C_{31} & C_{32} & C_{33} & & & \vdots \\ \vdots & & & \ddots & & \vdots \\ C_{n1} & & & & C_{nn} & 1 \\ 1 & 1 & \cdots & \cdots & 1 & 0 \end{bmatrix} \begin{bmatrix} \lambda_1 \\ \lambda_2 \\ \vdots \\ \vdots \\ \lambda_n \\ \mu \end{bmatrix} = \begin{bmatrix} C_{01} \\ C_{02} \\ \vdots \\ \vdots \\ C_{0n} \\ 1 \end{bmatrix} \qquad (2.36)$$

2.5.3 Sequential Gaussian Simulation

Kriging has several limitations, like smoothness of the kriging result, the lack of information for representing local uncertainty, unable to reproduce extreme values, and the underestimation of variance. To address some of the limitation of kriging, we can generate multiple realizations that conditioned on variogram and observed data using Sequential Gaussian Simulation (SGSIM).

The general procedure for SGSIM is

1. Select a random path.
2. Perform Kriging
3. Draw a sample from the Gaussian distribution of the kriging results and add it to data
4. Move to the next point in the random path and repeat the above procedure until one realization is generated

To generate another realization, repeat the above procedure.

2.6 The K-SVD Algorithm

When using a sparse constraint to regularize an ill-posed history matching problem, it is common to use generic transformation method like Discrete Cosine Transform (DCT) and Discrete Wavelet Transform (DWT). Even through these methods are general and easy to implement, it is hard to take the geology nature of the problem and the prior information into consideration by using DCT or DWT. K-SVD, one more effective and specialized method of constructing sparse base is recently developed

(Aharon et al. 2006) and applied into history matching problem (Khaninezhad et al. 2010). Based on the geostatistical simulation methods such as Sequential Gaussian Simulation and Sequential Indicator Simulation, we can generate an ensemble of realization that are consistent with the prior information on the reservoir. With these prior realizations, we can construct a K-SVD dictionary. And this dictionary can be used in the sparse transformation to regularize the inverse problem. Since the dictionary is constructed from the prior information and the geology nature of the problem, it is more effective in the inverse problem than previous transformation methods.

K-SVD is a generalization of the K-means algorithm. In K-means algorithm, a set of vectors is learned, and each sample will be represented by only one of these vectors by assigning the sample to its nearest neighbor. The K-means method may be regarded as an extreme sparse representation in which only one element in the dictionary is taken to decompose the sample. In this way, the corresponding coefficient has to be one. The K-SVD can be viewed a generalization of K-means in that the combination of multiple dictionary elements can be used to represent the sample. Then, the number of non-zero element does not have to be one even though it is still sparse. And the coefficients of these elements don't have to be one. Sparse K-SVD bases can be generated from an ensemble of realizations that are consistent with the prior knowledge of the reservoir.

In K-SVD, the training of the dictionary can be done by the minimization of the following problem (Aharon et al. 2006).

$$\min_{D,X}\{\|Y - DX\|_F^2\} \tag{2.37}$$

subject to

$$\|X_i\|_0 \leq T_0 \tag{2.38}$$

for all i.

In the K-SVD method, the minimization can be done iteratively (Aharon et al. 2006). The first step is using pursuit algorithm like matching pursuit and the orthogonal matching pursuit algorithm to find the approximate optimal coefficient matrix$X$. One advantage of K-SVD is that all pursuit method as long as it can provide a solution with a determined number of non-zeros elements. In the first step, the Dictionary D will remain fixed. The second step is the searching of a better dictionary. The main difference of the step from other method is that K-SVD update one element as well as it's correspond coefficient in the dictionary at one time. All other elements remain fixed during this process. The update of one element in the dictionary has a straight forward solution based on the singular value decomposition (SVD). In addition, the update of dictionary element and its coefficient simultaneously improve the speed and stableness of convergence process. Carrying out the above two steps iteratively until the convergence criteria is meet will give a K-SVD learned dictionary. The detailed theory, implementation procedures, and experiments can be found in Aharon's discussion (Aharon et al. 2006).

2.7 Sparse Regularization

In the process of history matching, because of the overwhelming number of unknowns and the limited number of observations, the inverse problem is usually ill

posed. That is, there are more than one set of unknown values can explain the observed data equally well. To solve this problem, we need to add prior information on the reservoir properties to regularize the problem. Because of the geology nature of the problem, the reservoirs properties are usually show a certain extent of continuity over spatial domain. So we can apply this spatial continuity as regularization to the inverse problem. One way to apply this continuity is to use prior variogram model of the reservoir properties to obtain the covariance between every set of two grid blocks. Then, we can use this generated covariance matrix to regularize the inverse problem as shown in the MAP estimation part of this paper. Another way to take the spatial continuity of reservoir properties into consideration is to apply a sparsity constraint into the inverse problem (Jafarpour et al. 2010). Li and Jafarpour (Li and Jafarpour 2010) applied the iteratively reweighted least-squares method into sparse regularized history matching problem. This method is effective and efficient in solving the subsurface heterogeneous inverse problem and works well in the DCT and DWT domain.

The sparse reconstruction problem can be expressed by

$$\min_{\mathbf{m}} \|\Phi \mathbf{m}\|_0 \tag{2.39}$$

Subject to

$$\|\mathbf{d_{obs}} - \mathbf{g}(\mathbf{m})\|_2^2 \leq \sigma \tag{2.40}$$

where Φ is a transformation basis such as DCT or DWT. $\sigma$is the measurement error variance.

This is a constraint minimization problem in which we want to find the set of parameter $\mathbf{m}$ which can explain the observed data with the observation error and has the

minimum number of non-zero elements in the sparse transformation domain. However, the direction solution of this problem is impossible because of the solution require an exhaustive search over the whole possible parameter space. The extensive computation effort required to do this asks one to think about equivalent formulation to this problem. One approximate solution is to applying a convex relaxation and then solves the resulted optimization problem.

$$\min_{\mathbf{m}} \|\Phi\mathbf{m}\|_p^p \tag{2.41}$$

subject to

$$\|\mathbf{d_{obs}} - \mathbf{g}(\mathbf{m})\|_2^2 \leq \sigma \tag{2.42}$$

One equivalent expression of this constrained optimization problem is as the following,

$$\min_{\mathbf{m}} \boldsymbol{J}(\mathbf{m}) = \|\mathbf{d_{obs}} - \mathbf{g}(\mathbf{m})\|_2^2 + \lambda\|\Phi\mathbf{m}\|_p^p \tag{2.43}$$

That is, the regularized inverse problem can be solved by the minimization of an objective function which incorporates a sparse constraint term to the ill-posed observation misfit term with a parameter λ that balance the weight between the sparsity $\|\Phi\mathbf{m}\|_p^p$ and the observation misfit term.

According to Li and Jafarpour (Li and Jafarpour 2010), this minimization can be solved by an iteratively reweighted method as the following

$$\boldsymbol{J}(\mathbf{m}) = \|\mathbf{d_{obs}} - \mathbf{g}(\mathbf{m})\|_2^2 + \lambda\|\Phi\mathbf{m}\|_{\mathbf{W}}^2 \tag{2.44}$$

where $\|\Phi\mathbf{m}\|_{\mathbf{W}}^2 = \mathbf{m}^T\Phi^T\mathbf{W}\Phi^T\mathbf{m}^T$. And the weighting matrix $\mathbf{W}$ is a diagonal matrix that that place less weight on the sparse term at early iterations and larger weights on the sparse term at later iteration.

At each iteration when solving this problem, the diagonal elements of the matrix $\mathbf{W_{i,i}} = [(\Phi \mathbf{m}^k)_i^2 + \boldsymbol{\varepsilon}^k]^{\frac{p}{2}-1}$ where $\boldsymbol{\varepsilon}^k = \|\mathbf{d_{obs}} - \mathbf{g}(\mathbf{m})\|_2^2$ is a small parameter that to avoid the singularity of the matrix and adaptively control the weighting matrix during the iterations. A detailed discussion and derivation of the matrix $\mathbf{W}$ can be found in Li's discussion (Li and Jafarpour 2010).

The Newton method can be used for the minimization of the objective function; we can update the unknown vector $\mathbf{m}$ at each iteration according to the following,

$$\mathbf{m}^{n+1} = [\mathbf{m}: \boldsymbol{\partial J^{n+1}}/\boldsymbol{\partial \mathbf{m}} = \mathbf{0}] \tag{2.45}$$

This approach was developed Li and Jafarpour (Li and Jafarpour 2010) with DCT and DWT transformation and implemented into the K-SVD method by Khaninezhad et al. (2010). Effectiveness of the sparse constraint was demonstrated in two Dimensional problems. When this sparse constraint method is done with the K-SVD dictionary, we can make a change on the notation to make the expression simpler. Let α stands for the representation of the unknown parameters to be estimated in the K-SVD transformation domain, and $\mathbf{D}$ be the K-SVD trained dictionary which will transform the K-SVD representation to the spatial domain.

That is

$$\mathbf{m} = \mathbf{D}\alpha \tag{2.46}$$

So that the objective function to be minimized can be rewritten as

$$\boldsymbol{J}(\alpha) = \|\mathbf{d_{obs}} - \mathbf{g}(\mathbf{D}\alpha)\|_2^2 + \lambda\|\alpha\|_{\mathbf{W}}^2 \tag{2.47}$$

Its minimization can be done in a way similar to the optimization of the problem before.

The determination of the weight parameter λ is a little hard, and the current procedure for determine its value including L-curve method and the generalized cross validation method.

CHAPTER III

MODEL SETUP AND EXPERIMENT RESULTS

3.1 Model and Experiment Setup

We use a synthetic non-isothermal three-dimensional single phase flow system in the experiment. The governing equations are solved using the finite difference method to obtain the pressure and temperature at each grid cell. A fully implicit formulation is used to solve the governing equations. The sensitivity of observations with respect to the reservoir properties are obtained by adjoint method. The covariance matrix of the prior permeability and conductivity can be obtained from the prior information on variogram model.

The detailed properties of the reservoir model can be found in Table 3-1 through Table 3-3.

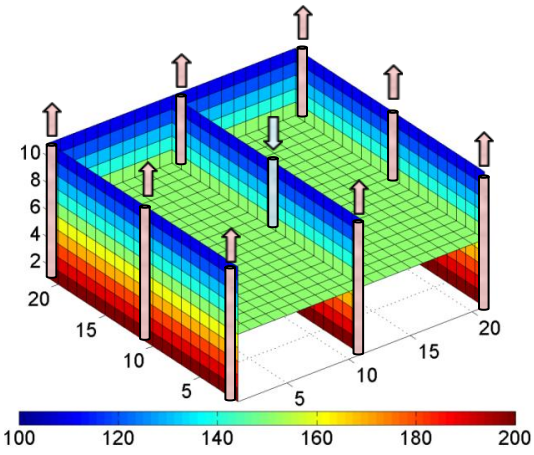

Figure 3-1. Initial Temperature Distribution

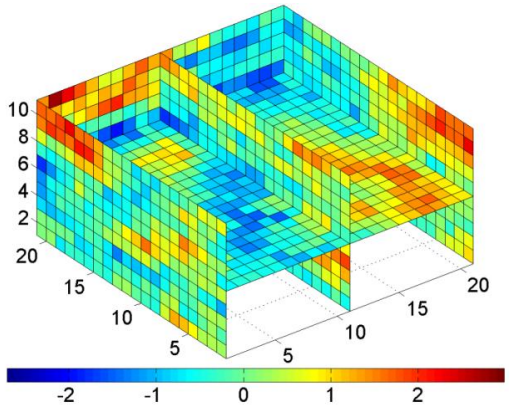

Figure 3-2. True Permeability Distribution

The initial temperature on the top layer of the reservoir is 100 °C and that on the bottom layer is 200 °C. The geothermal gradient is assumed to be constant within the reservoir. Water at about room temperature (20 °C) is injected through the injection well in the middle of the reservoir and water is produced at eight production wells as shown by Figure 3-1. The configuration of the reservoir model and the initial temperature distribution is given by Figure 3-1 and Figure 3-2. Figure 3-3 shows the placement of temperature sensors.

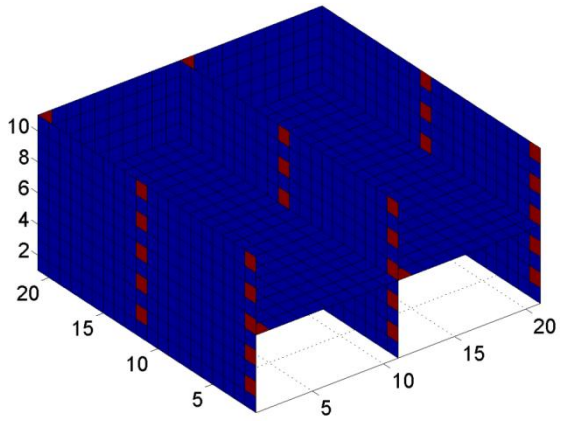

Figure 3-3. Temperature Sensor Placement

The observations are pressure at injection well, production rate and temperature at two production wells. The observation is taken from the exact result of the forward simulation run but the relative observation error is taken as 2 % for pressure measurement and temperature measurement to generate the observation covariance

matrix C_D. In the experiment, we assume measurements are independent to each other so that C_D is a diagonal matrix.

Table 3-1 Discretization parameter, initial, boundary conditions, and general parameters

Properties	Values	Properties	Values
Simulation Time	1000 Days	Observation Interval	50 Days
Reservoir Dimension	$1260 \times 1260 \times 660$ feet	Grid System	$21 \times 21 \times 11$
Cell Dimension	$60 \times 60 \times 60$ feet	Initial Pressure	2920 psi
Boundary Conditions	No Flow Boundaries	Production Rate Error	2 %
Production Temp Error	2 %	Injection Pressure Error	2 %
Gravity	0 m/s^2 (Neglected)	Temp Sensor Error	2 %

Table 3-2 Well setup

Properties	Values	Properties	Values
Number of Injectors	1	Production Well Radius	0.583 feet
Number of Producers	8	Production Well BHP	2900 psi
Well Index Model	Peaceman's Model	Injection Observation	Pressure
Total Injection Rate	66000 BBL/Day	Production Observation	Rate and Temperature
Injection Temperature	20 °C		

The injection well injects evenly at each grid block at a total rate of 66000 BBL/Day along the vertical direction. The production rate at each well is a summation of the production rate with a constant bottom hole pressure of 2900 psi at each grid block along the vertical direction. And the production temperature is the rate weighted mean of

the production temperature at each production grid block. The well index of the production well is obtained from Peaceman's model (Peaceman 1978).

Table 3-3 The properties of rock and fluid

Properties	Values	Properties	Values
Rock Porosity	0.2	Fluid Compressibility	3×10^{-6} (1/psi)
Rock Heat Capacity	0.84×10^3 J/K	Expansion Coefficient	207 $(10^{-6}/°C)$
Rock Density	2.7×10^3 kg/m^3	Reference Pressure	2800 psi
Fluid Reference Density	1×10^3 kg/m^3	Reference Temperature	20 °C
Fluid Heat Capacity	4.19×10^3 J/K	Fluid Viscosity Model	Likhachev's Model

The liquid properties in the experiment are taken as the properties of water. The fluid viscosity is calculated using Likhachev's model (Likhachev 2003).

Table 3-4 SGSIM parameters

Properties	Values	Properties	Values
Kriging Type	Ordinary Kriging	Nugget Effect	0
Max Conditioning Data	12	Permeability Sill	1 $\ln^2(mD)$
Search Ellipsoid Ranges	21×21×6	Conductivity Sill	0.09 $W^2/(m\cdot K)^2$
Search Ellipsoid Angles	0×0×0	Permeability Mean	1 $\ln(mD)$
Variogram Model	Spherical	Conductivity Mean	3 $W/(m\cdot K)$

The logarithm of true permeability map and the true conductivity map are generated by drawing two samples from the sequential Gaussian simulation based on the variogram parameter from Table 3-4. SGeMS (Remy et al. 2008) software which is the

Stanford Geostatistical Modeling Software developed at Stanford University is used for SGSIM.

3.2 MAP Estimation Results

The permeability characterization results using various observations are presented by Figure 3-4. We can see that the posterior permeability map characterized only on production rate (the 2nd column) shows homogeneity along the vertical direction. However, when conditioned on production temperature (the 1st and 3rd column), the posterior permeability shows a lot of heterogeneity along the vertical direction, and this heterogeneity is consistent with the true permeability map. This means production temperature conveys information on the vertical distribution of reservoir property and production rate convey information on the horizontal distribution of reservoir property. This can be interpreted as the following, because of the geothermal gradient, the temperature on the upper layer of the reservoir is much lower than that on the lower layer of the reservoir. So if the permeability on the upper layer is high, more hot water will be produced and this results in a higher production temperature, and vice versa. In this way, by observing the production temperature, we can tell how much water is from the upper layer and how much water is from the lower layer. The sensitivity analysis on the last two rows can further demonstrate this point. From the sensitivity analysis, we can see that the sensitivity of production rate have the same sign along vertical direction while those of production temperature have opposite signs. By

charactering permeability on both production rate and production temperature, we can get the best estimation of the permeability map (1st column).

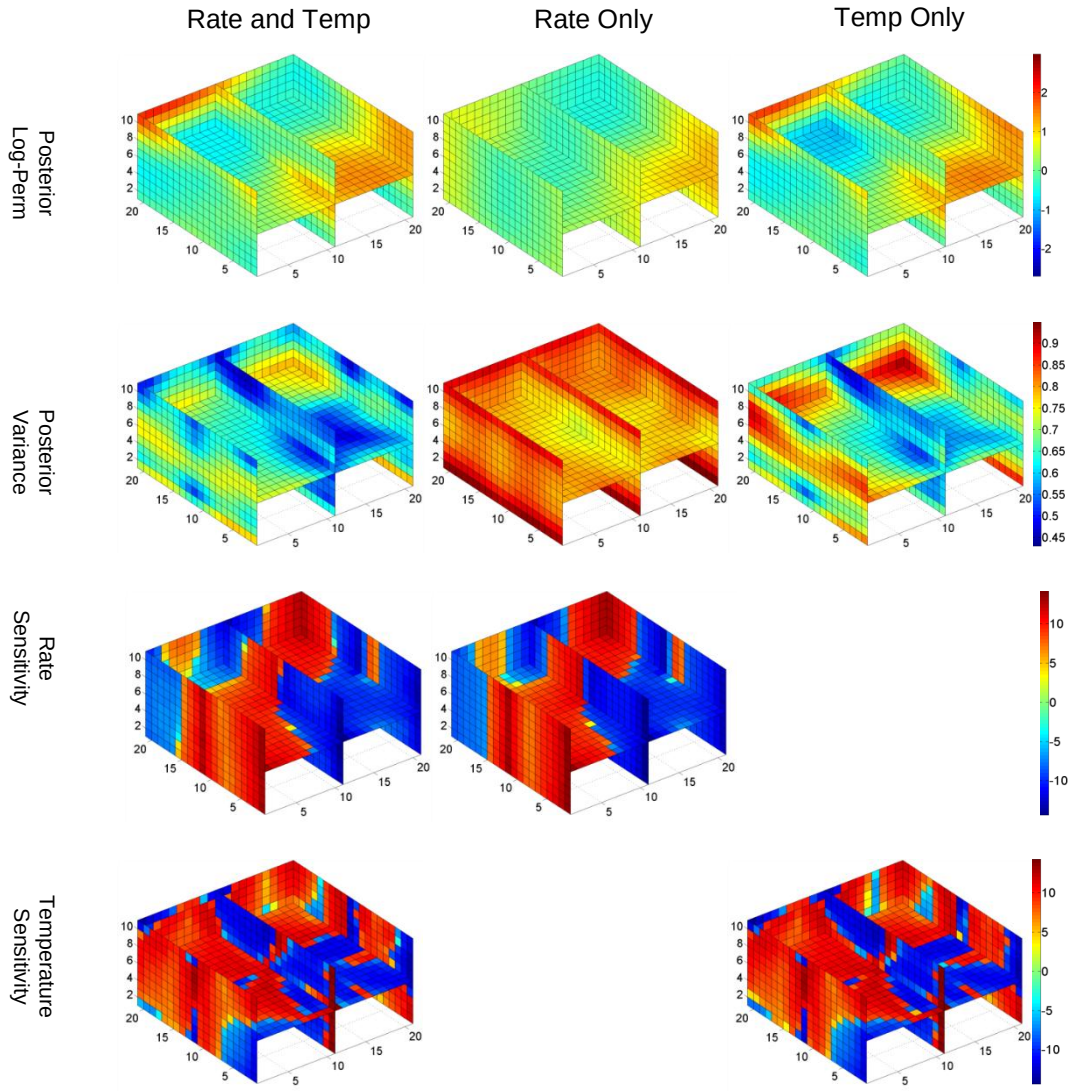

Figure 3-4. Comparison of Characterization Results Conditioned on Various Observations

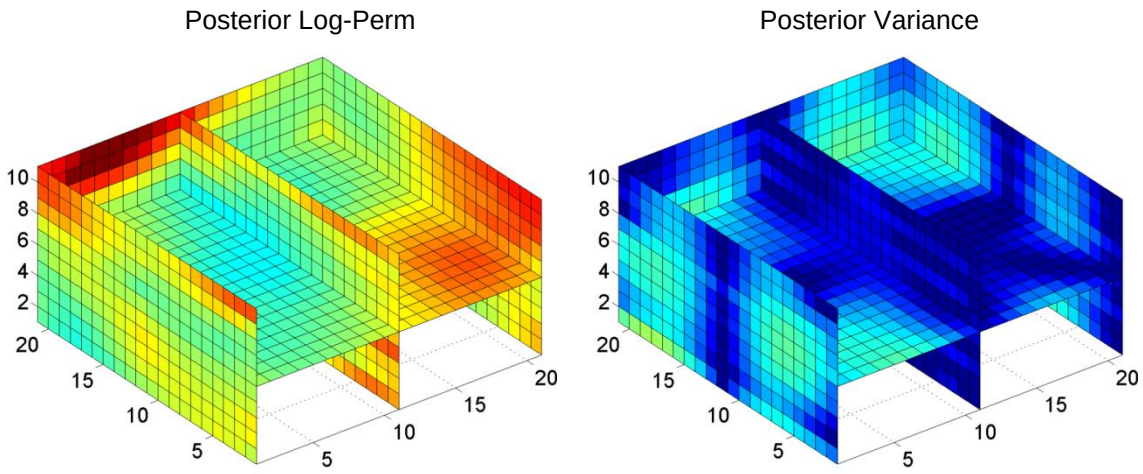

Figure 3-5. MAP Characterization Result with Downhole Temperature Sensors

The data match of the production data at well 1 is presented by Figure 3-6.

The production data of the prior reservoir model differs significantly from the observed production data. However, when the model is characterized on production rate or both production rate and production temperature, the predicted production rate matches the observed production rate very well. When the model is characterized on production temperature or both production rate and production temperature, the predicted production temperature has a good match with the observed production temperature.

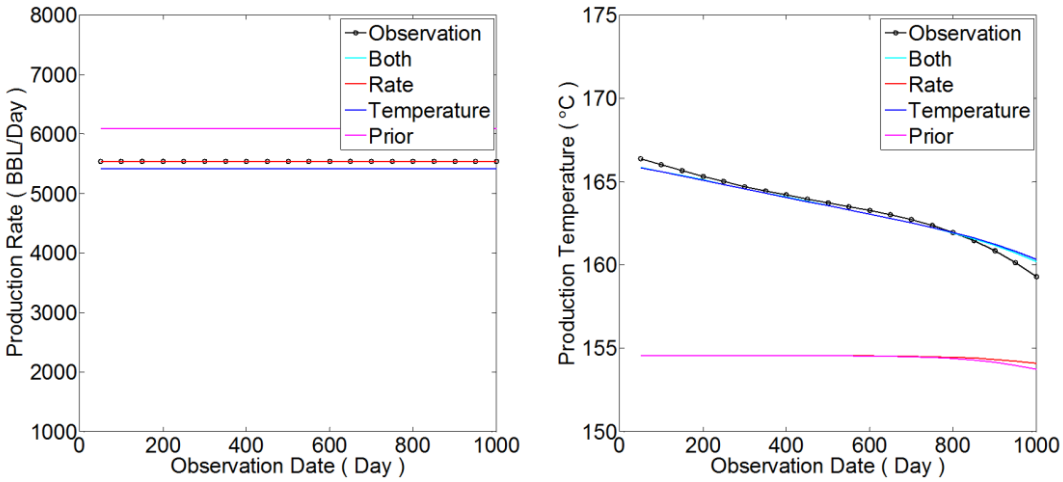

Figure 3-6. Production Data Match of Maximum A Posterior Characterization

To study the effect of the data from downhole temperature sensors such as fiber optic sensor on characterization, we proposed a model with permanent downhole distributed fiber optic sensors as shown as Figure 3-3. The results characterization result is presented by Figure 3-5. The posterior permeability distribution is more heterogeneous than those without downhole temperature sensors, this is because these temperature sensors are vertically distributed and thus carry information on the vertical distribution of reservoir properties.

3.3 RML Estimation Results

However, the MAP estimation gives only one realization of the posterior probability density function. In addition, it is under the assumption of Gaussian distribution and linearity of the model. In realistic case, these assumptions are usually

untrue. So instead of MAP estimation, we can use RML to generate multiple realizations of history matched models for uncertainty analysis and risk assessment. The RML estimation of the reservoir is done with a realization number of 100. The characterization results are shown as the following. Similar to the MAP estimation, the RML also give a pretty good characterization results. In addition, the multiple realizations dawned by RML make uncertainty analysis possible. Unlike the posterior variance of the MAP estimation which gives a smaller variance at the well locations, the uncertainty of the RML estimation is more uniform.

Three randomly selected realizations are shown by Figure 3-8. Every posterior permeability distribution presents more similarity with the true permeability distribution comparing to the prior one.

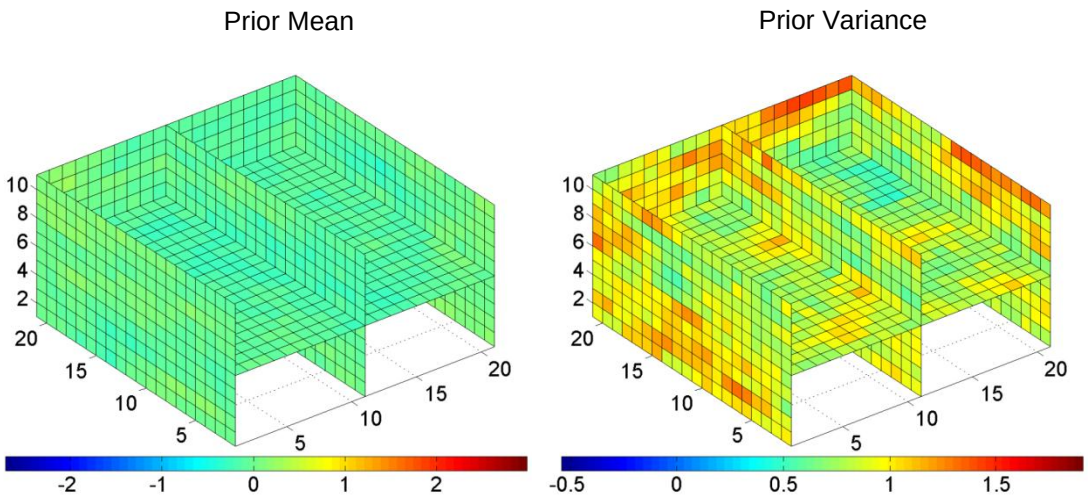

Figure 3-7. Randomized Maximum Likelihood Characterization Results

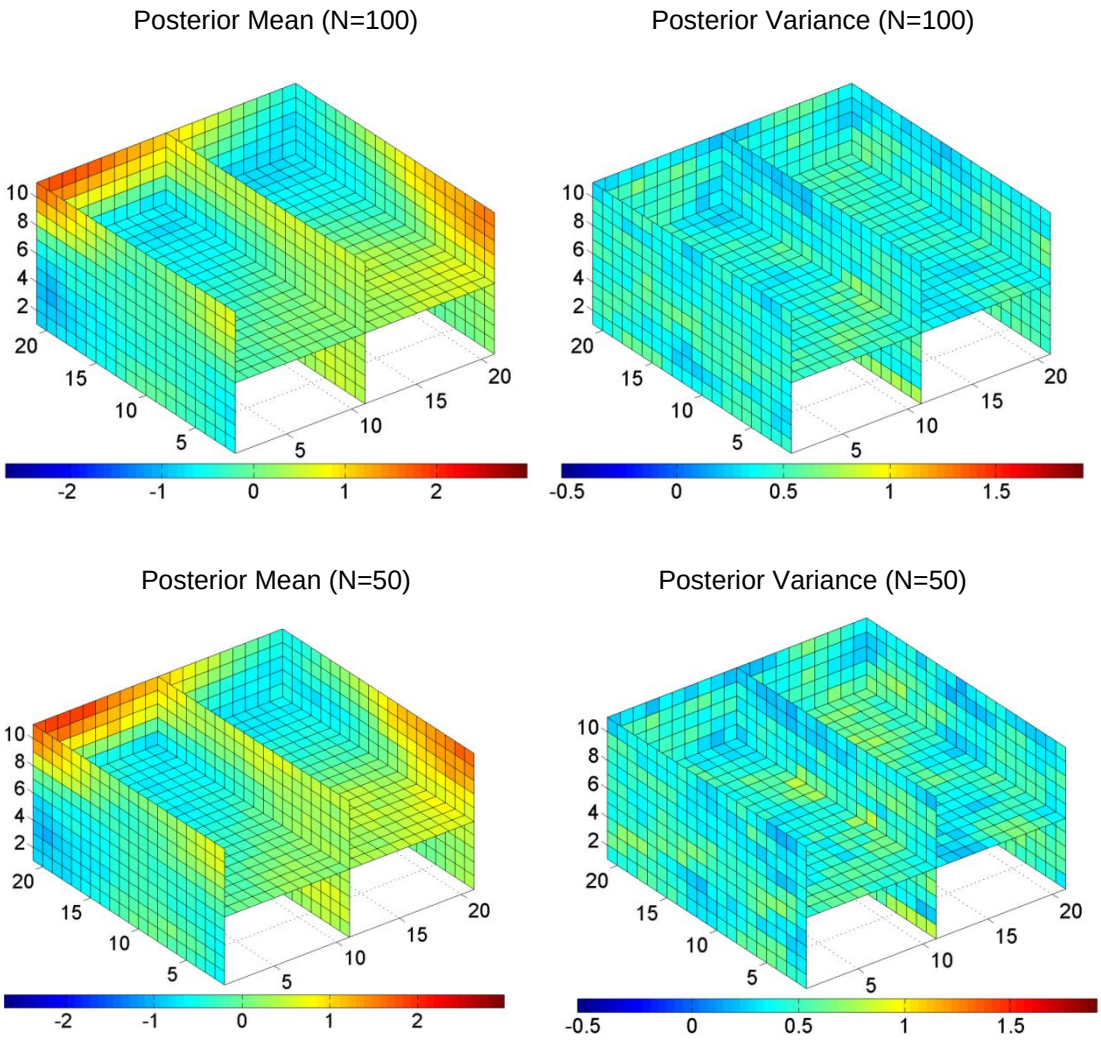

Figure 3-7. Continued

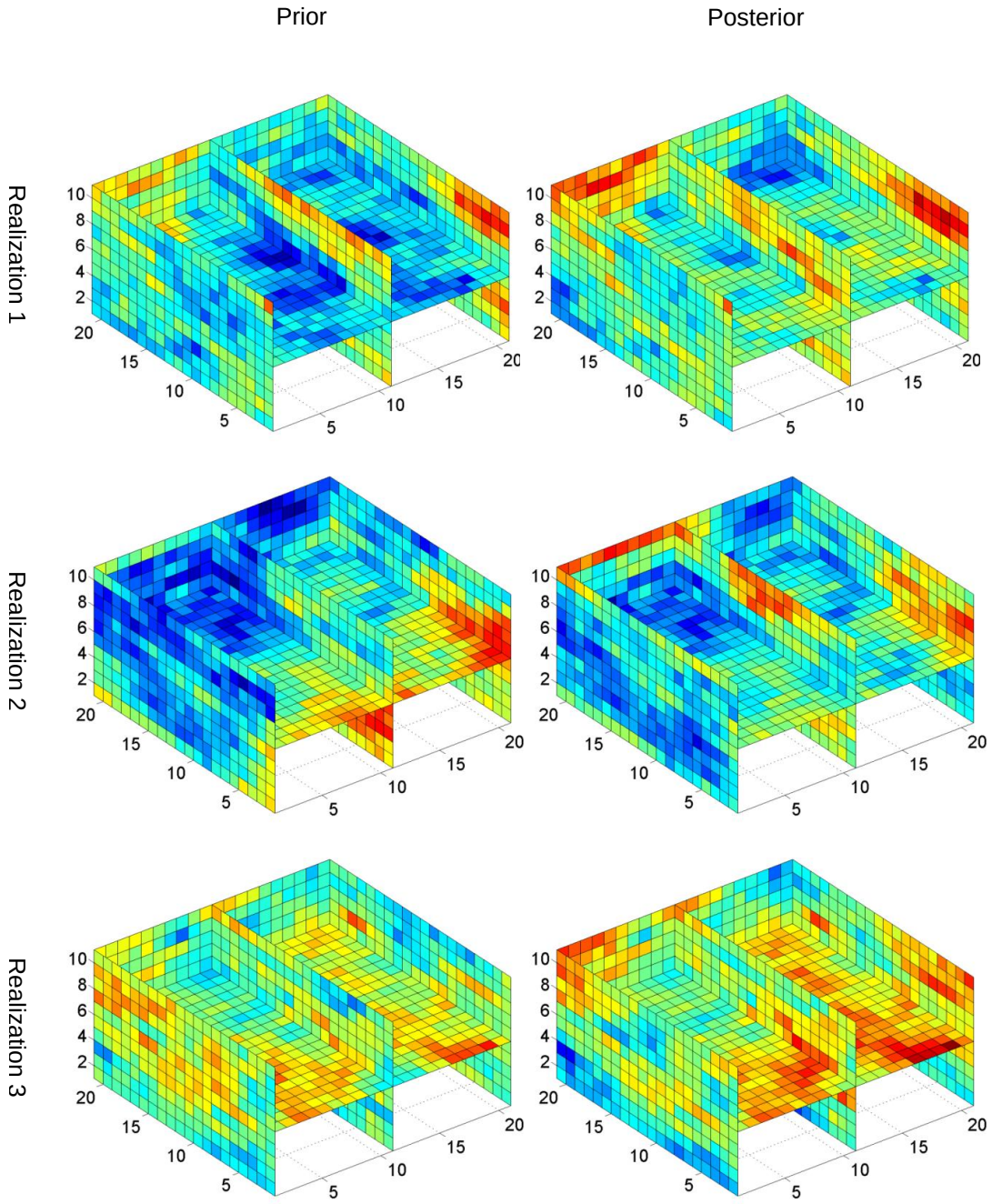

Figure 3-8. Sample Realizations of Randomized Maximum Likelihood Characterization

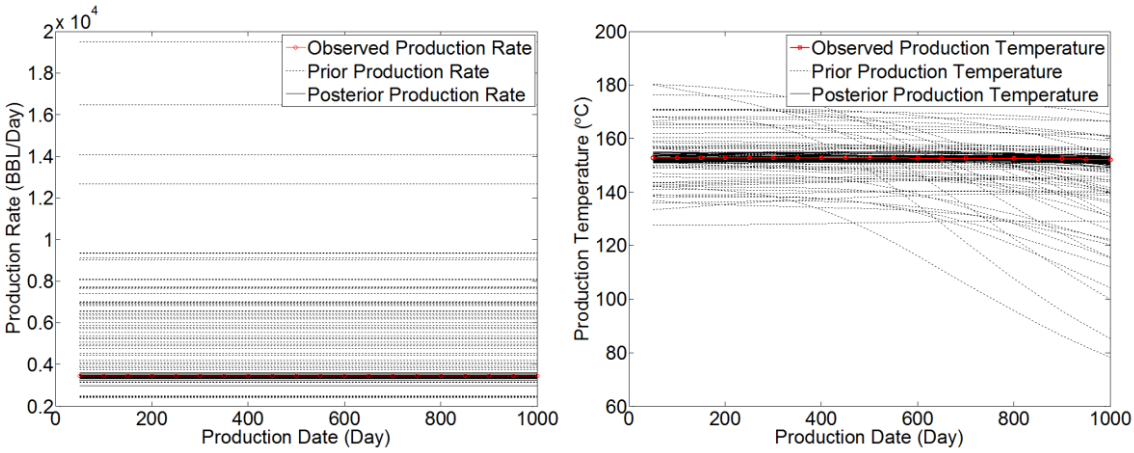

Figure 3-9. Production Data Match of Randomized Maximum Likelihood Characterization

The data match for production rate and production temperature is shown in Figure 3-9. The production rate and production temperature of the prior realizations significantly differs from the observed production data. As expected, the production data converges to the observed production data after the RML estimation.

To verify that 100 is a sufficient number of realizations for RML characterization, we studied the effect of the number of realizations on posterior permeability and standard deviation. We used 50 realizations in the RML and the result including posterior permeability and posterior standard deviation is similar with that with 100 realizations. The requirement of number of realizations comparing to number of unknown parameters to be estimated is so small is because the correlations between each pair of unknown parameters, especially adjacent parameters are very strong.

3.4 K-SVD Estimation Results

Before the process of optimize the objective function, we need to specify the parameter λ which regularize the weight between the data misfit and the sparsity. The determination of a proper value of parameter λ is not simple. The proper value of λ depends on the accuracy and availability of the observation data, the number of the dictionary elements, the sparsity of the problem and the specific property the reservoir. So the proper value of λ is case by case and cannot be determined before the actual process of characterization. The methods for determining λ including L-curve (Hansen 1999) and the generalized cross validation (GCV) methods. These methods are computationally inefficient. Li and Jafarpour (Li and Jafarpour 2010) proposed a multiplicative regularization method that multiply the regularization term to the data misfit term thus avoid the problem of determining parameter λ. In the paper, we still use the normally additive regularization method and experiment on the effect of parameter λ on the sparsity and accuracy of the characterization results. We plotted the characterization results and K-SVD transformation coefficients for various λs.

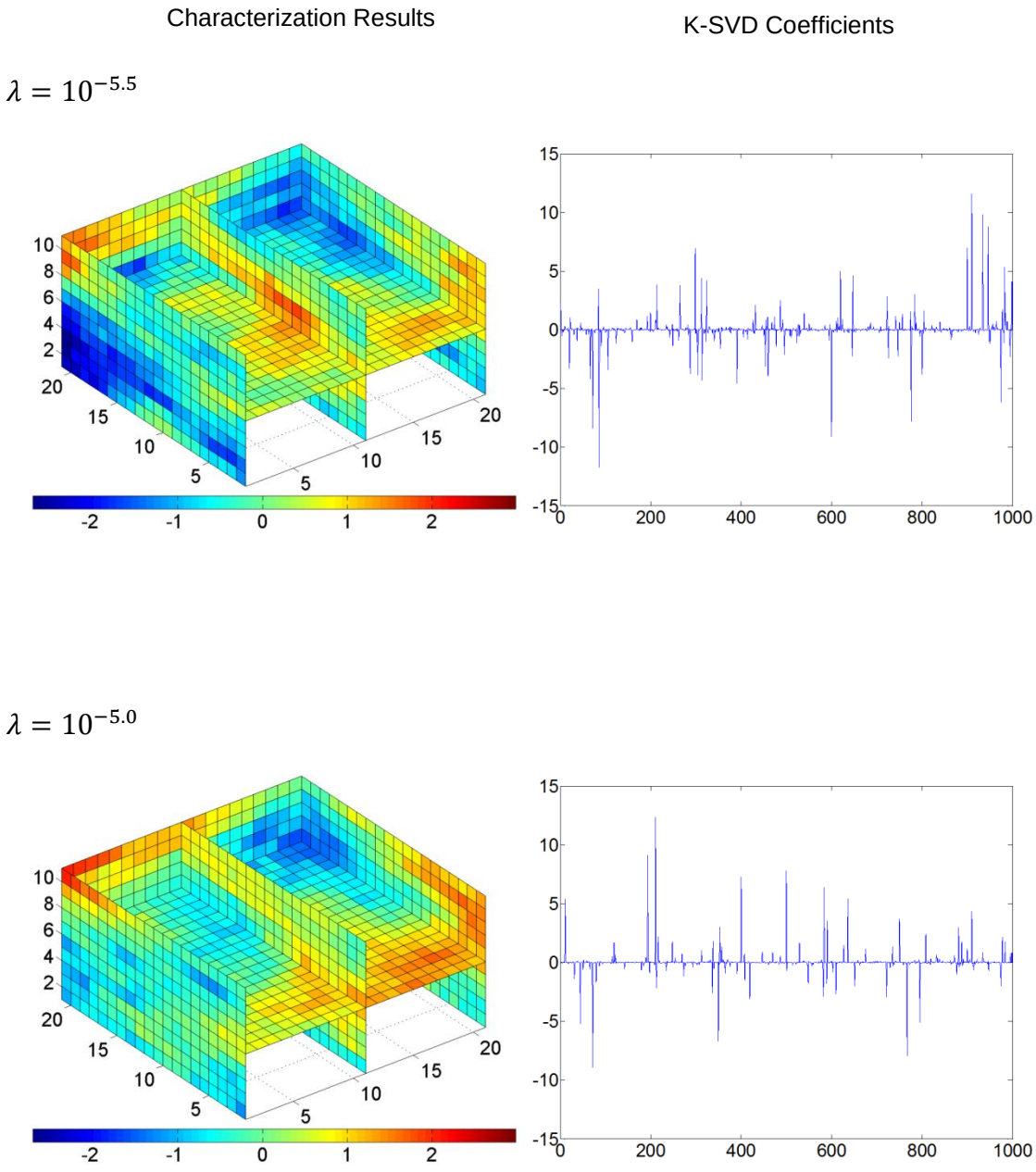

Figure 3-10. K-SVD Constrained RML Results with Various λs

$\lambda = 10^{-4.5}$

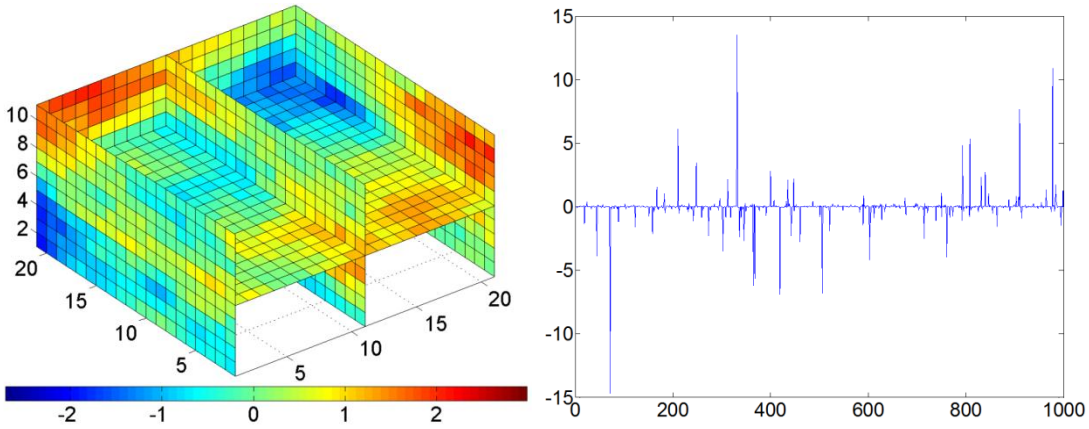

$\lambda = 10^{-4.0}$

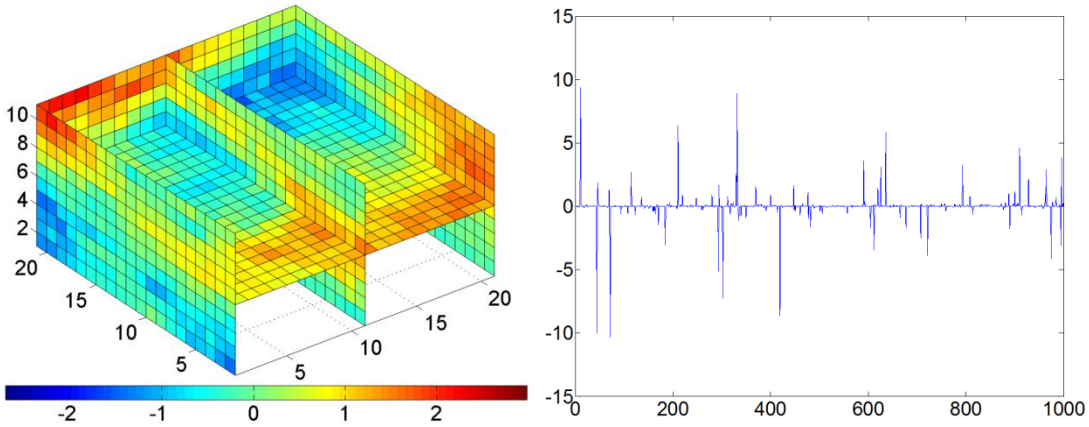

Figure 3-10. Continued

$\lambda = 10^{-3.5}$

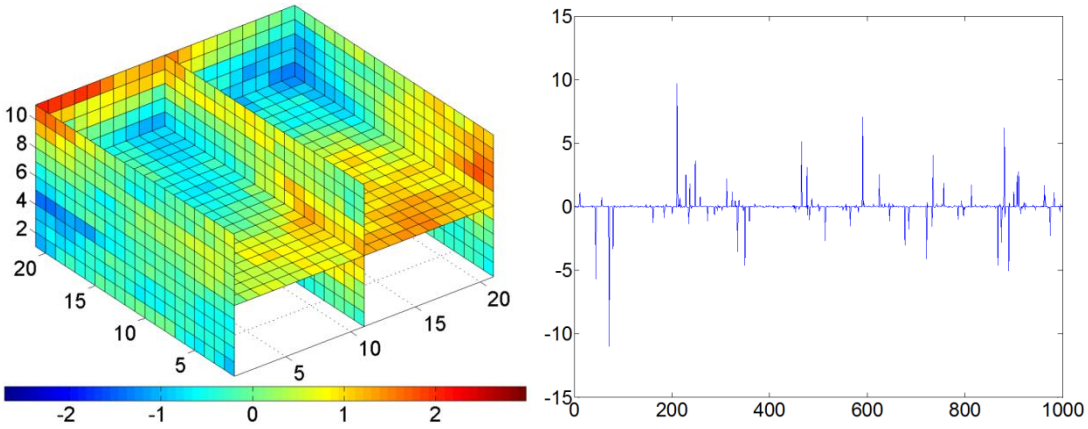

$\lambda = 10^{-3.0}$

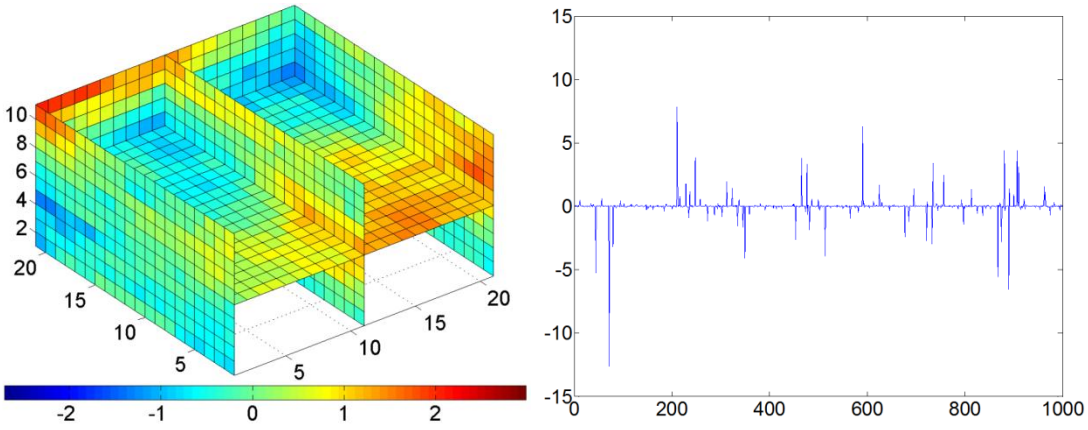

Figure 3-10. Continued

$\lambda = 10^{-2.5}$

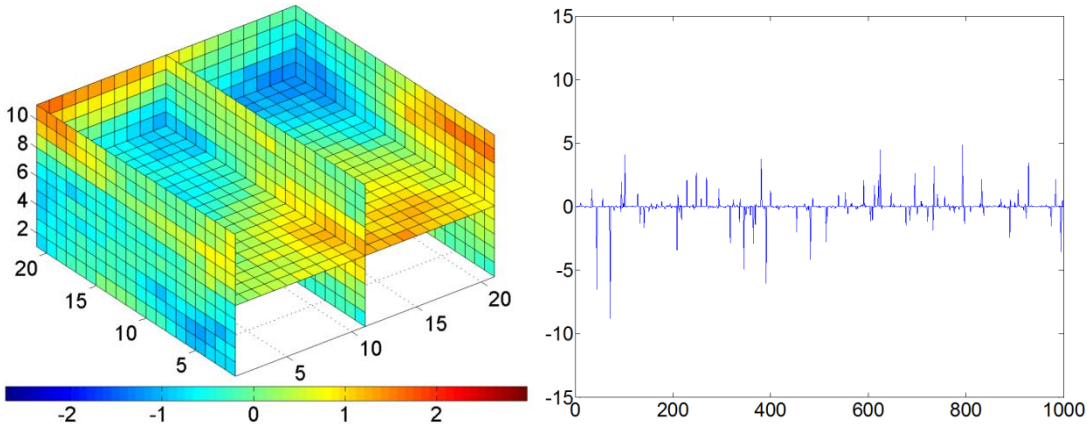

$\lambda = 10^{-2.0}$

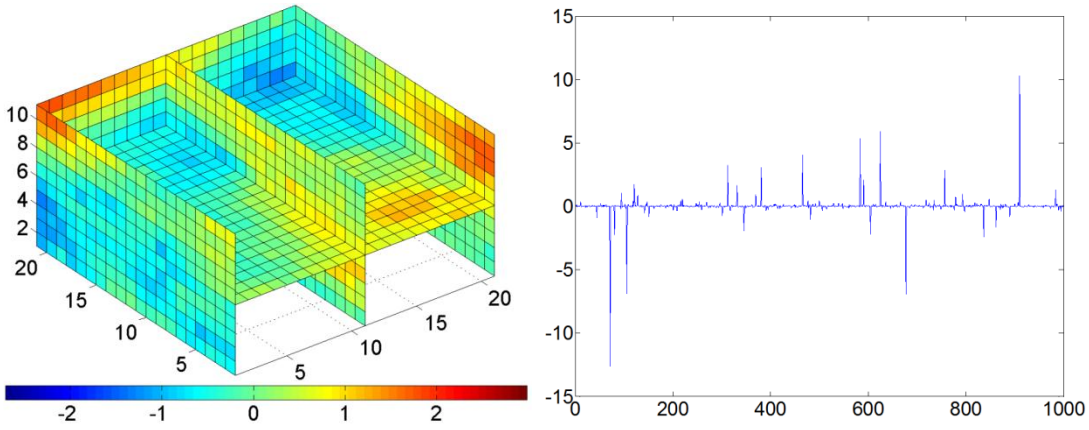

Figure 3-10. Continued

$\lambda = 10^{-1.7}$

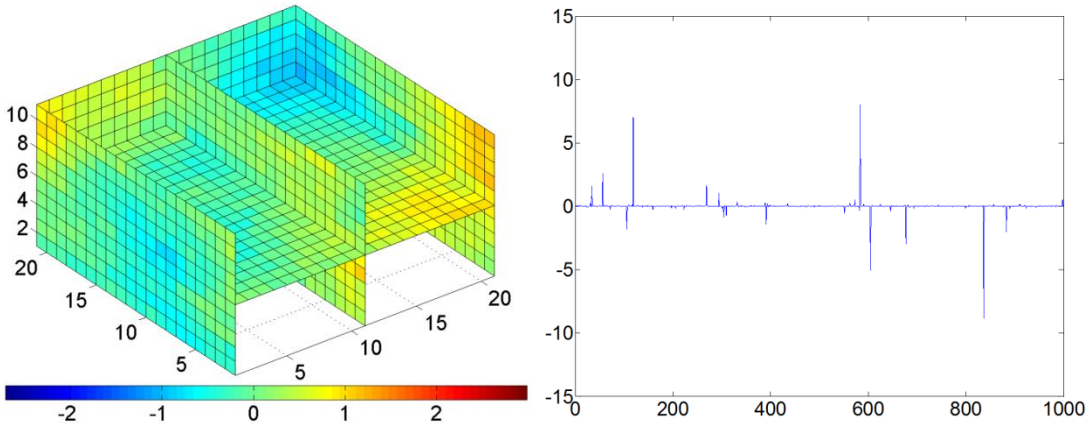

Figure 3-10. Continued

As the value of the parameter λ increases, the sparsity increases, that is the number of non-zero elements of the reconstruction results in K-SVD transformation domain decreases. This is because larger λ put more weight on the sparsity of the result. And the characterization result will be smoother and less variance in the spatial domain.

In addition, we plotted the dependence of data misfit of reconstructed results on the value of the parameter λ. When of value of the $\log_{10}\lambda$ is in the range of -4.5 to -1.5, the data misfit is approximately a monotonic increasing function of the parameter λ. And the data misfit is pretty small in the range of -4.5 to -3.0.However, the data misfit goes larger when the value of $\log_{10}\lambda$ goes below -4.5. This is because of the ill-condition of the matrix in the process of the minimization of the objective function. The value of the sparsity, that is the l_1-norm of the K-SVD coefficients, as a function of the value of the $\log_{10}\lambda$ is shown in Figure 3-11. This is a monotonic increasing function

since the larger λ will put more weight on the sparsity term. The best value of λ is a trade-off between the data-misfit and the sparsity. Here, based on the analysis of the reconstruction results, we take $\log_{10}\lambda = -3$ is all of the following experiments.

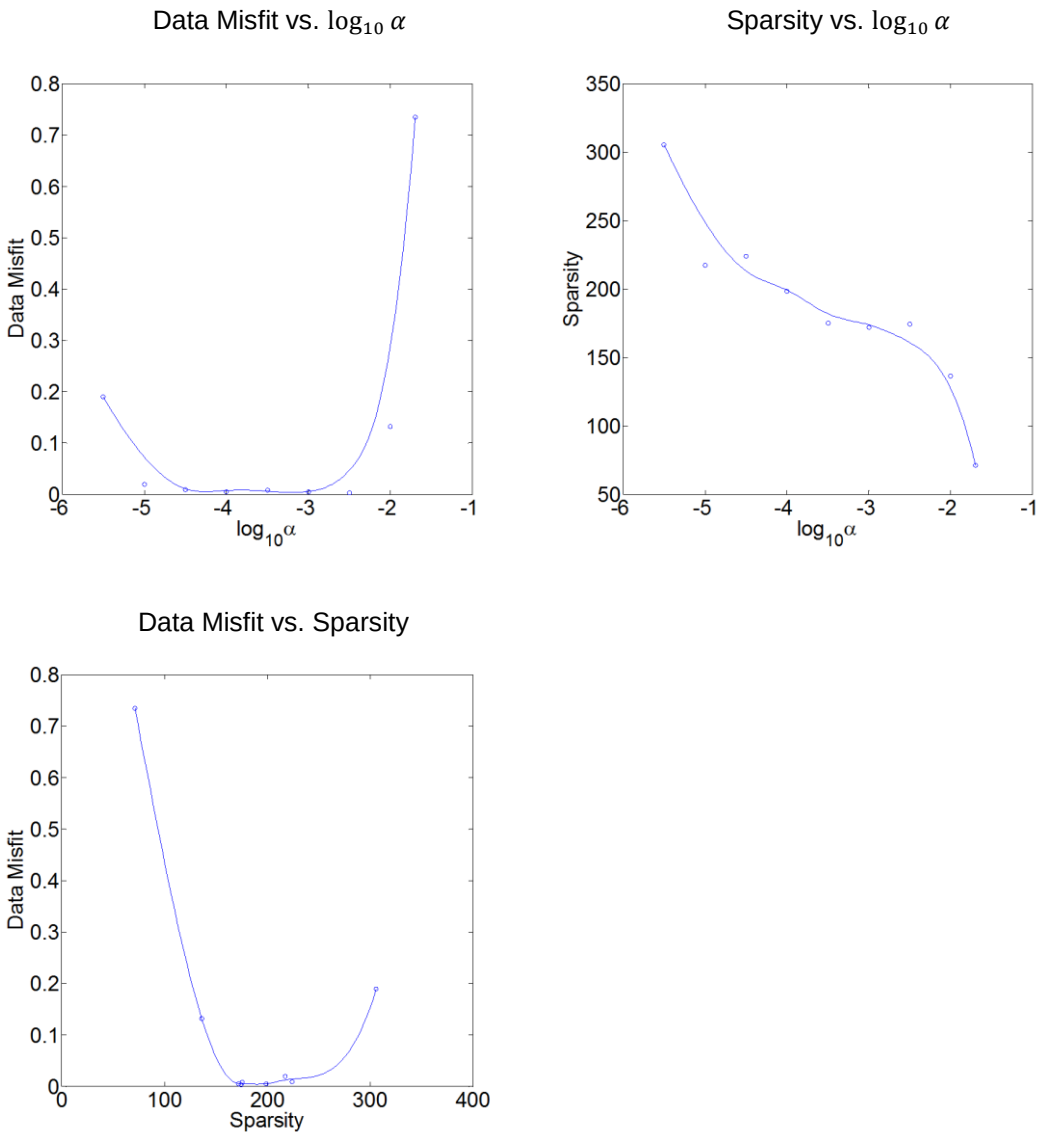

Figure 3-11. Data Misfit and Sparsity of Characterization Results with Various αs

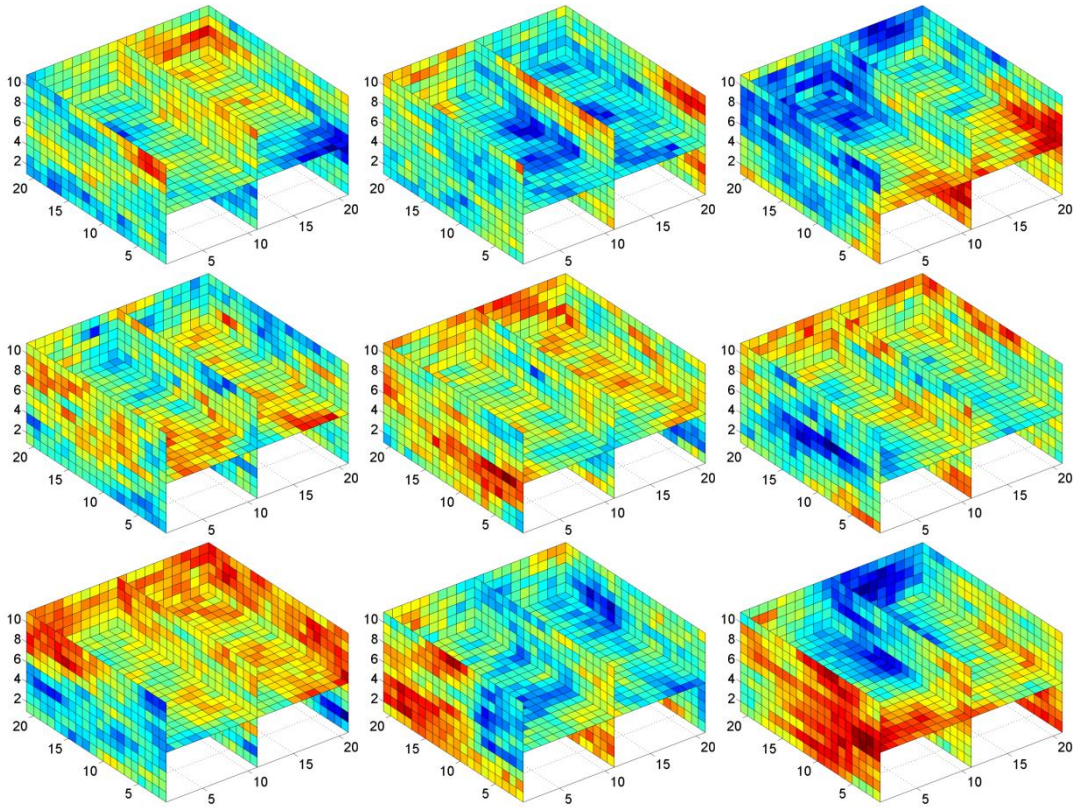

Figure 3-12. K-SVD Dictionary Training Samples

Then we apply the regularization using the K-SVD basis. The training samples were generated using Sequential Gaussian Simulation using the same parameters with the RML example. The number of training samples is 1500 and they are consistent with the true permeability distribution that we want to reconstruct. This consistence makes the comparison between K-SVD constrained RML method and regular RML possible. 9 of the training samples are shown in Figure 3-12. The variance among these 9 realizations is a representation of the uncertainty of prior knowledge.

Dictionaries with element number $K = 1000$ and sparsity $S = 25$, with $K = 1000$ and $S = 50$, with $K = 500$ and $S = 25$, with $K = 500$ and $S = 50$, and with $K = 250$ and $S = 25$ are trained with these 1500 training samples.

We make a comparison on the characterization results using different K-SVD dictionaries with various dictionary sizes and sparsities. All the initial permeability distribution is uniform over the whole space. The results are shown as Figure 3-13.

Example1 K = 1000, S = 25

K-SVD Dictionary Elements

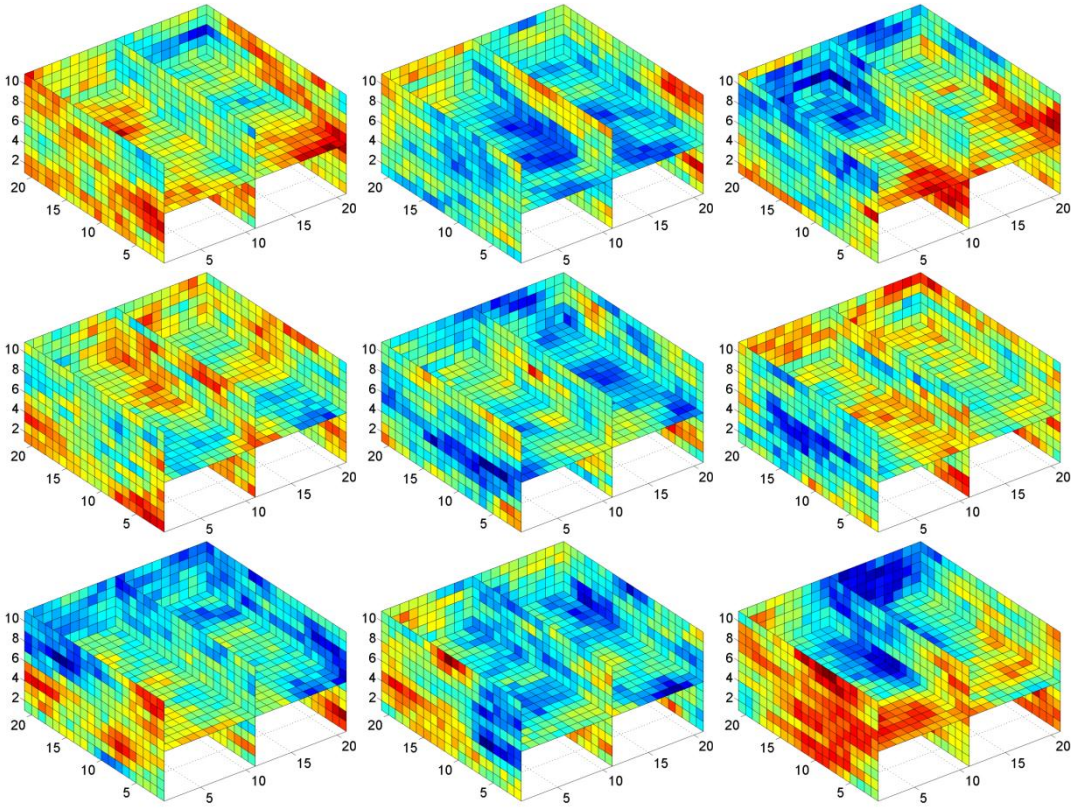

Reconstruction Results

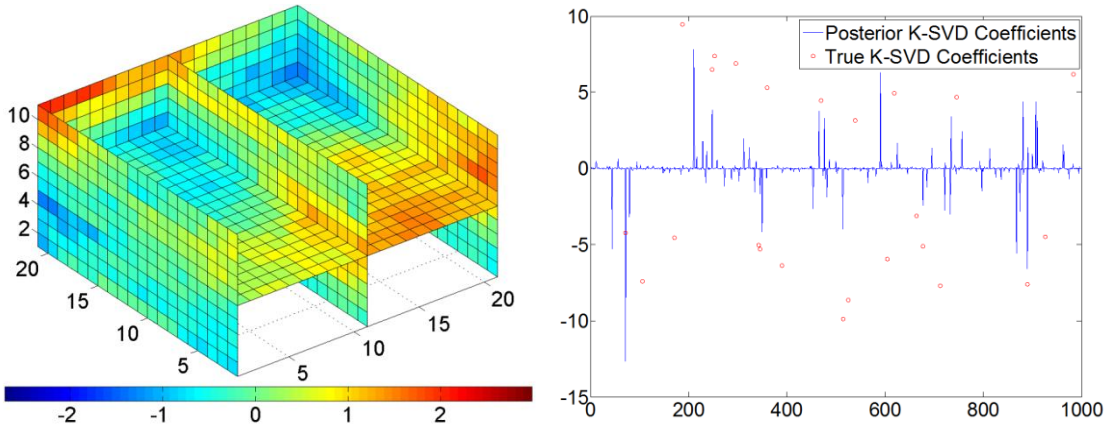

Figure 3-13. Characterization Results of Various K-SVD Dictionaries

Example1 K = 1000, S = 5

K-SVD Dictionary Elements

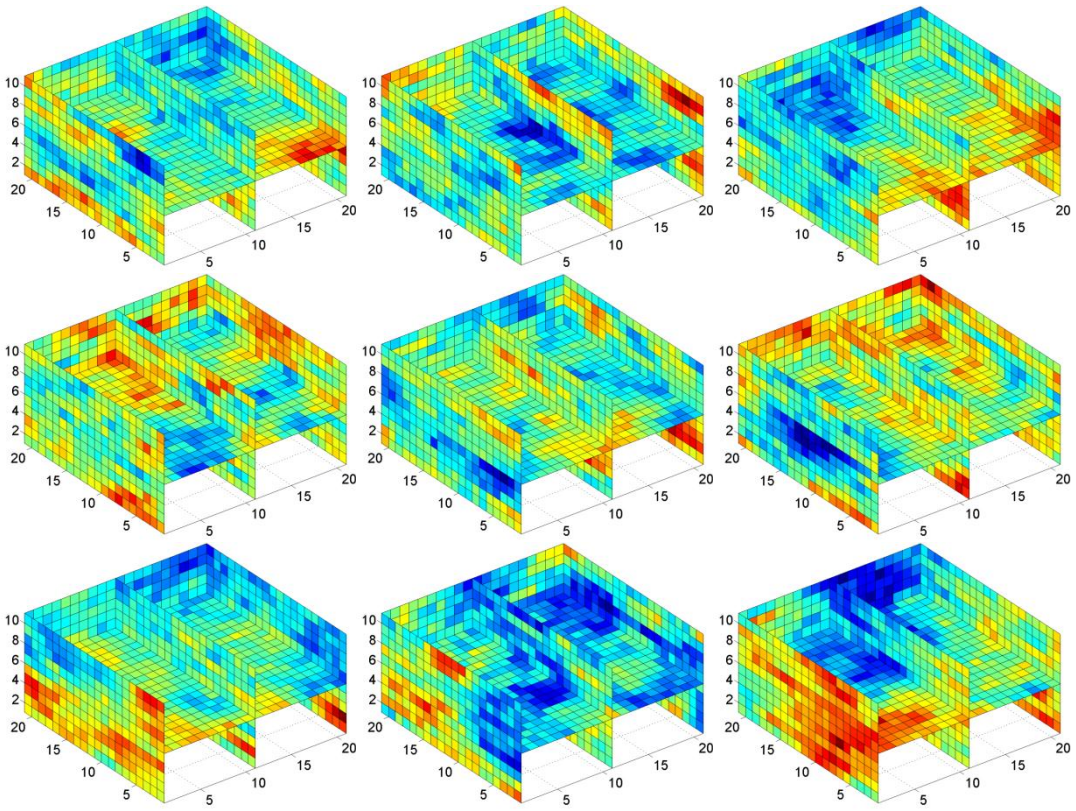

Reconstruction Results

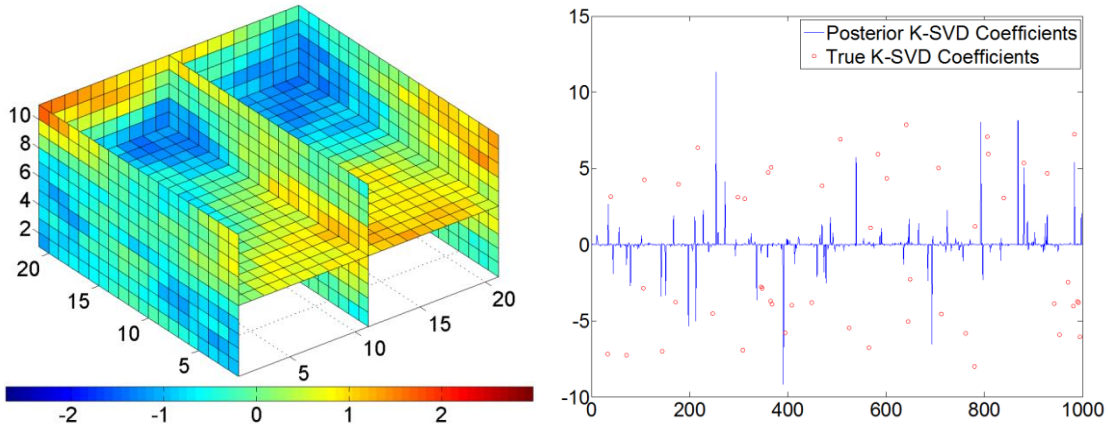

Figure 3-13. Continued

Example1 K = 500, S = 25

K-SVD Dictionary Elements

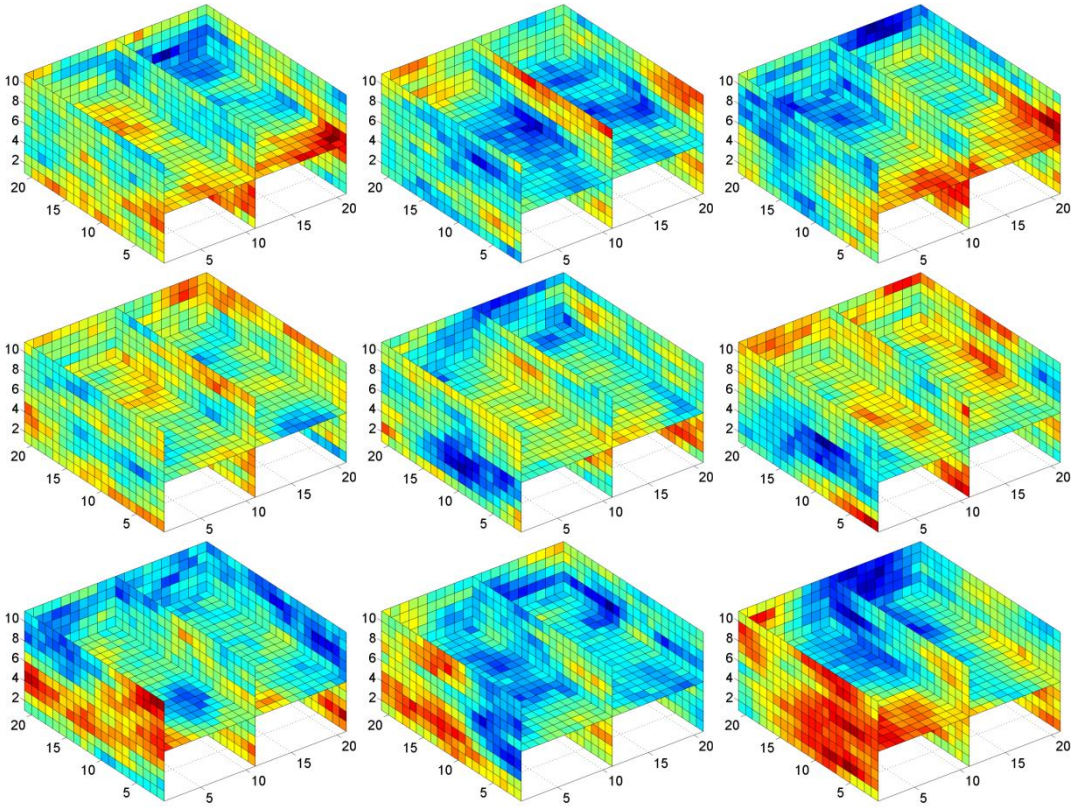

Reconstruction Results

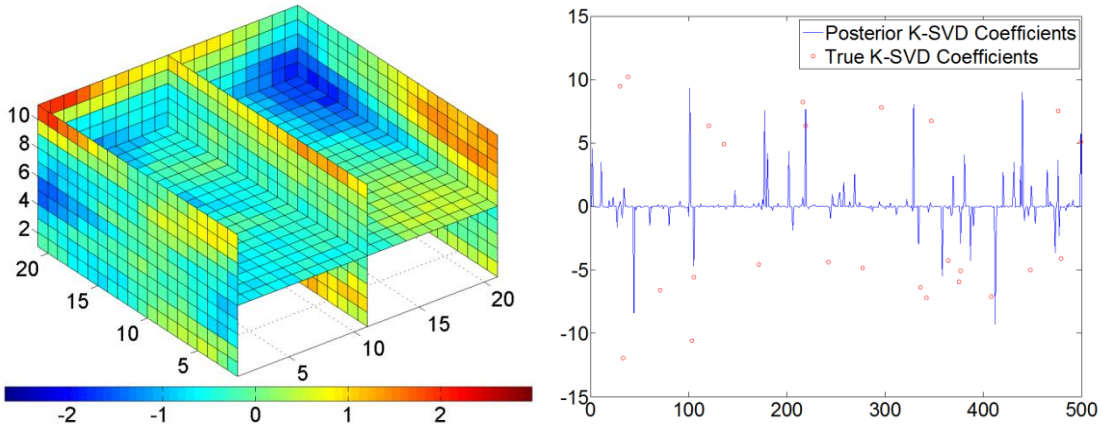

Figure 3-13. Continued

Example1 K = 500, S = 50

K-SVD Dictionary Elements

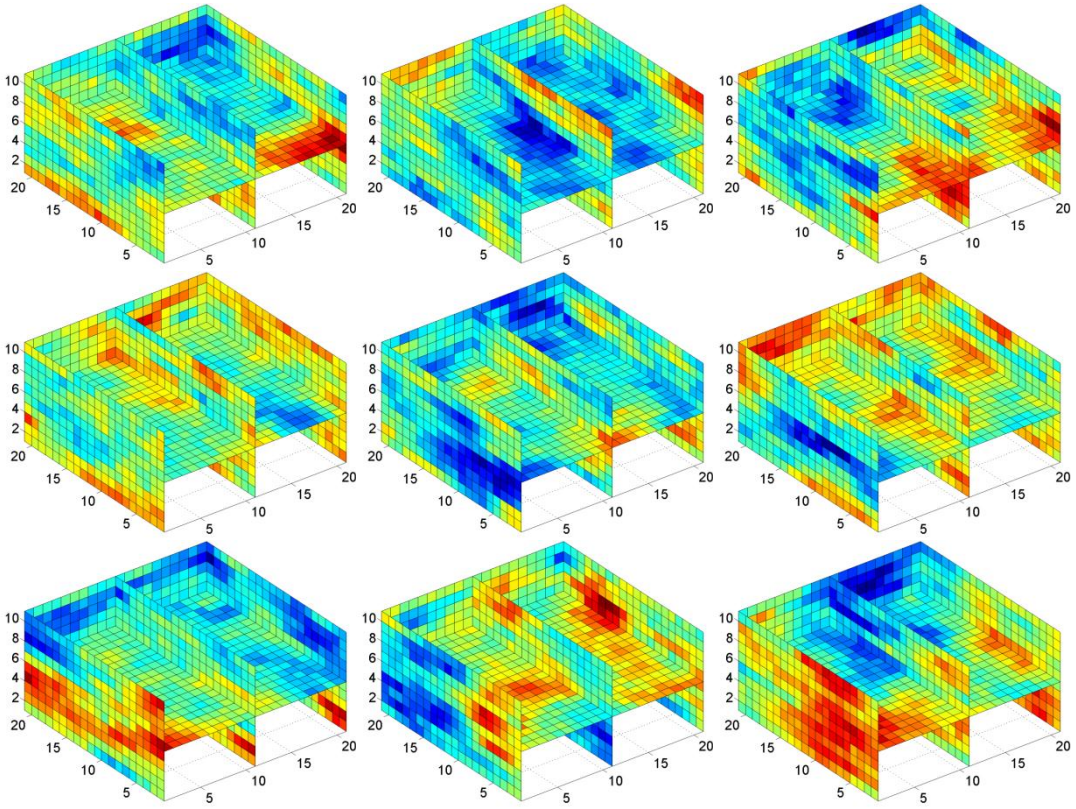

Reconstruction Results

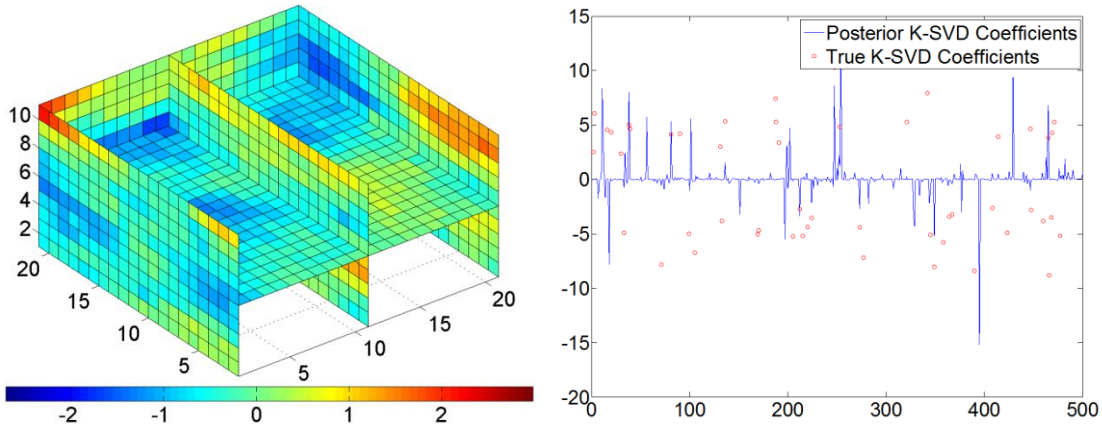

Figure 3-13. Continued

Example1 K = 250, S = 25

K-SVD Dictionary Elements

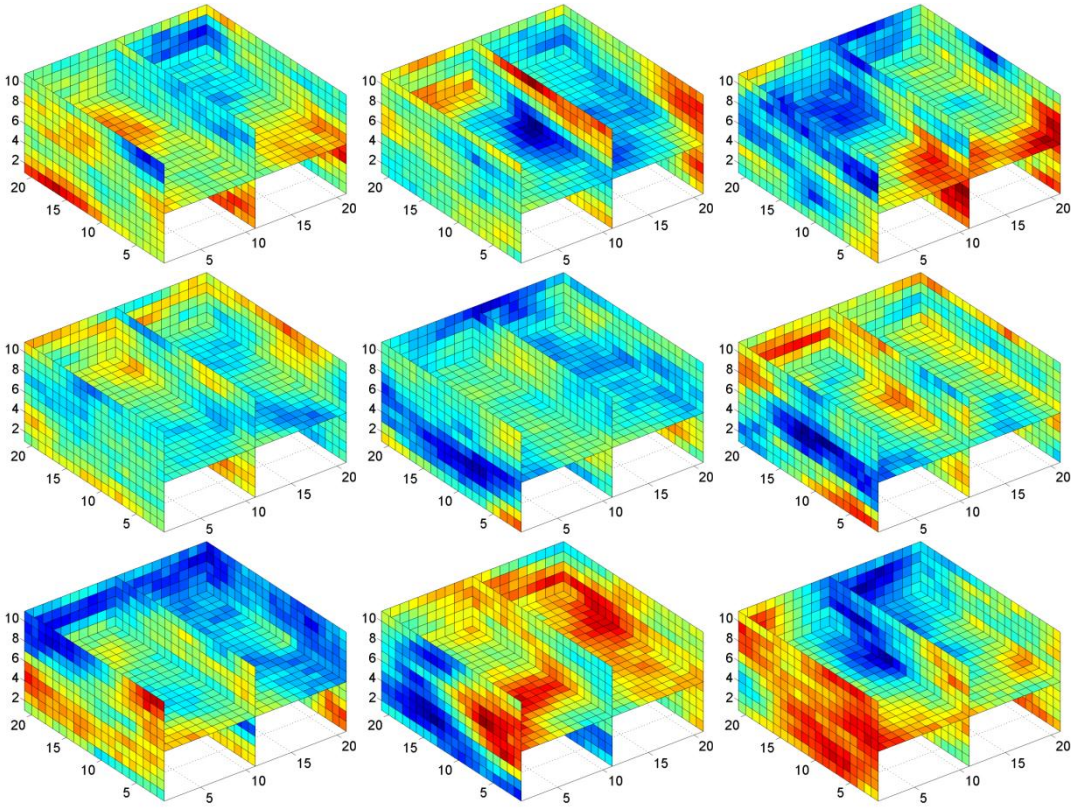

Reconstruction Results

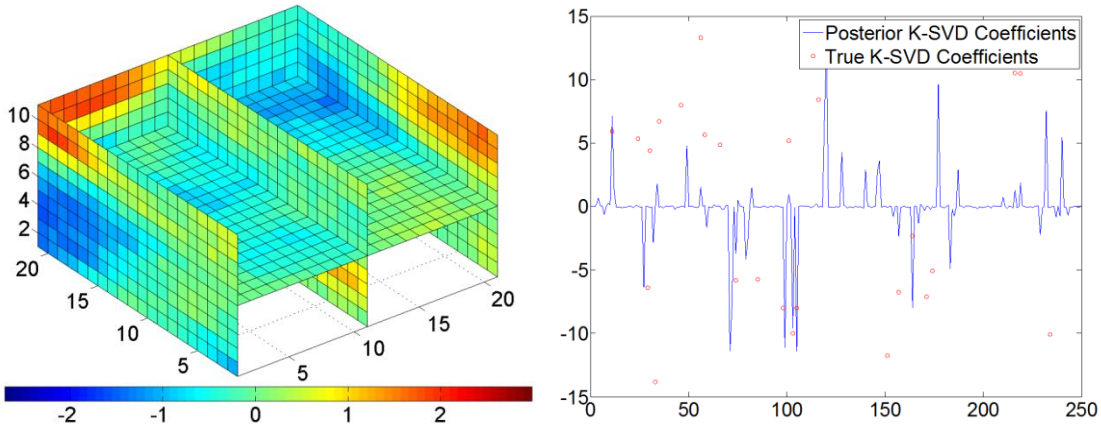

Figure 3-13. Continued

We can draw the same conclusion on our three dimensional non-isothermal reservoir model with Khaninezhad et al. (2010). That is, when the number of dictionary element is decreased, the smoothness of the dictionary elements will be increased. This means that we will put more weight on the covariance between grid block pairs in the process of reservoir characterization. Another advantage of reducing the number of dictionary elements is the increasing in the computation burden in the training of the dictionary. However, if the available data is enough, the continuity of the dictionary elements may result in the underestimation of the variance along the space. So choice of the dictionary element number is a tradeoff between the reconstruction diversity and reservoir connectivity base on the availability and accuracy of data and the property of the reservoir to be reconstructed.

3.5 K-SVD Constrained RML Estimation Results

Worse than the MAP estimation, the K-SVD method doesn't even give a estimation on the posterior variance of the reconstructed permeability distribution. So again we can use RML to generate multiple realizations of history matched models for uncertainty analysis and risk assessment. The K-SVD constrained RML estimation of the reservoir is done with a realization number of 100. The characterization results are shown as the following. The K-SVD constrained RML also give a pretty good characterization results and the posterior variance distribution as shown in Figure 3-14.

Three randomly selected realizations are shown by Figure 3-15. Every posterior permeability distribution presents more similarity with the true permeability distribution comparing to the prior one.

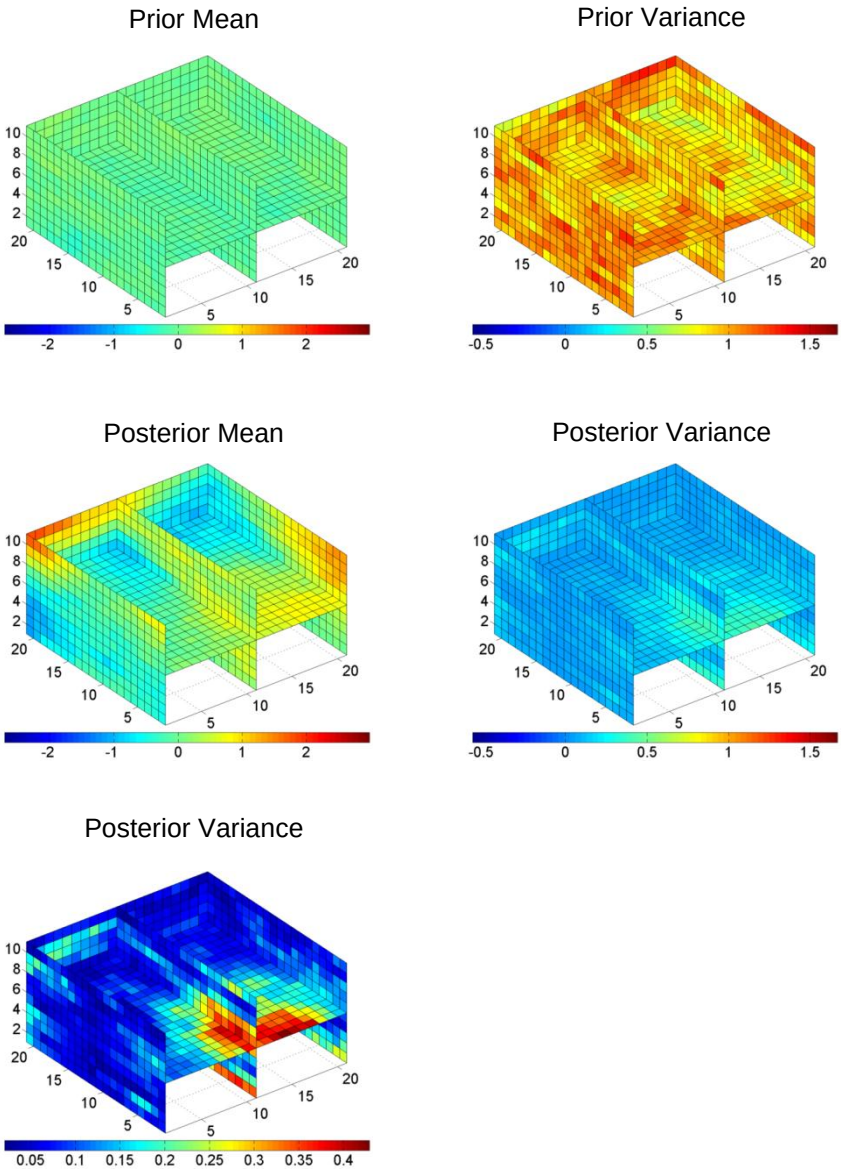

Figure 3-14. K-SVD Constrained RML Characterization Results

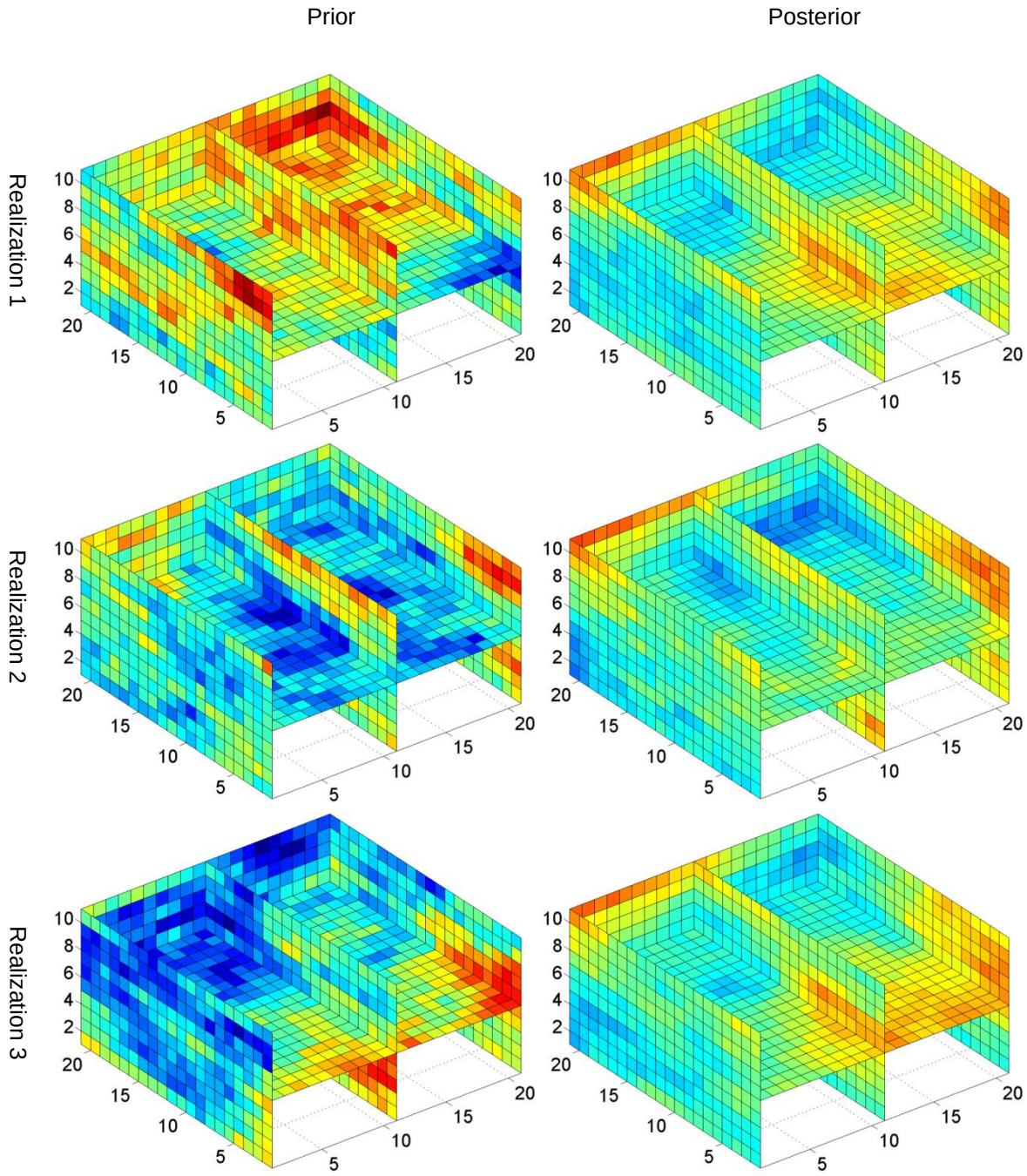

Figure 3-15. Sample Realizations of K-SVD Constrained RML

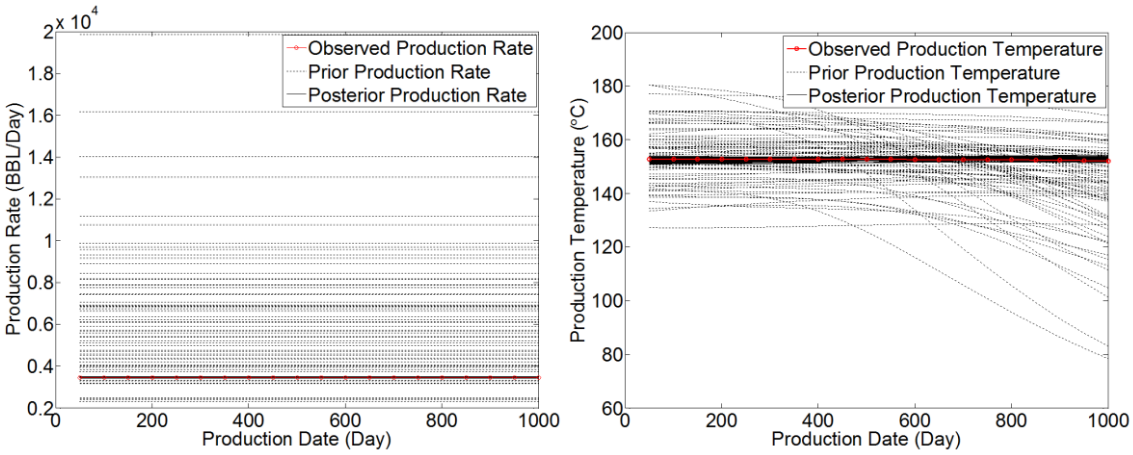

Figure 3-16. Production Data Match of Randomized Maximum Likelihood Characterization

CHAPTER IV

CONCLUSIONS

In this thesis, we studied the joint inversion of production and temperature data on the illumination of vertical permeability distribution in deep reservoirs. This reservoir characterization method takes both production rate and production temperature data into consideration for the inversion. The general idea behind taking production temperature into consideration is that the geothermal gradient results in temperature difference between various layers of the reservoir. The temperature difference makes temperature act as a kind of 'tracer' in the reservoir characterization. And the function of this 'tracer' is to identify the depth of the reservoir that the produced fluid comes from.

To achieve this goal, we first derived the governing equation for coupled fluid and heat flow which account for sources and sinks, viscosity dissipation, thermal expansion, heat convection and conduction. Then we built a non-isothermal reservoir simulator to simulate the fluid and heat flow in the reservoir. The adjoint method is incorporated into the simulator for efficient and accurate gradient calculation. The implementation of the adjoint method significantly reduces the burden of gradient calculation which is a barrier for fast reservoir characterization. Then, we use MAP estimation, RML estimation, K-SVD characterization, K-SVD regularized RML estimation separately to estimate the heterogeneous reservoir based on the only production rate, on only production temperature, and on both production rate and production temperature.

We used a three dimensional synthetic model to do the experiment. A full penetrating injection well is located at the center of the reservoir and eight full penetrating production wells are distributed uniformly on the boundaries of the reservoir. The permeability distribution is heterogeneity in the reservoir. The observations are production rate and production temperature and the unknown parameters to be estimated are the permeability at each grid block.

In MAP estimation, we use the prior variogram model to obtain the covariance between the permeability of each pair of grid block. With these covariance, we built a covariance matrix with ensure the smoothness of the posterior permeability distribution. The prior permeability distribution in MAP estimation is taken as a uniform distribution and the characterization results are consistent with the true permeability distribution. In RML estimation, we used 100 realizations and did the uncertainty analysis on the posterior permeability distribution. The variance of the posterior permeability is different from the predicted results of MAP estimation. As to the K-SVD estimation, we use dictionaries with various numbers of dictionary elements and different sparsity trained by K-SVD to do the estimation. The effect of K-SVD dictionary on estimation results are presented and analyzed. The K-SVD transform term act as a regularization term in the objective function. And a parameter λ is used to balance the weight of the sparisty of the results and the data match. We test the effect of the value of λ on the sparsity and the data misfit of the results. And the development of the results for various λ is shown. Again, we used the RML estimation to make the uncertainty analysis for K-SVD method.

We compared the characterization results on various observations. The comparison on reservoir characterization results conditioned on only production rate, only production temperature, both production rate and production temperature shows that production temperature indeed improve the result of estimation by conveying information on the vertical distribution of the reservoir permeability. . In addition, we made the sensitivity analysis which shows how the production results will change over a small change on the permeability at each grid block. This sensitivity further demonstrated this point.

REFERENCES

Aharon, M., Elad, M., and Bruckstein, A. 2006. K-SVD: An Algorithm for Designing Overcomplete Dictionaries for Sparse Representation. *IEEE Transactions on Signal Processing* **54** (11): 4311-4322. DOI:10.1109/TSP.2006.881199.

Arnold, G., Cavalero, S.R., Clifford, P.J. et al. 2010. Ss: Thunder Horse and Atlantis Deepwater Frontier Developments in the Gulf of Mexico: Thunder Horse Takes Reservoir Management to the Next Level. Paper OTC 20396 MS presented at the Offshore Technology Conference, Houston, Texas, 3-6 May. DOI: 10.4043/20396-MS.

Bejan, A. 2004. *Convection Heat Transfer*. New York City: John Wiley & Sons.

Bischof, C., Khademi, P., Mauer, A. et al. 1996. Adifor 2.0: Automatic Differentiation of Fortran 77 Programs. *IEEE Computational Science & Engineering* **3** (3): 18-32. DOI: 10.1109/99.537089.

Bischof, C., Roh, L., and Mauer-Oats, A. 1997. Adic: An Extensible Automatic Differentiation Tool for Ansi-C. *Software: Practice and Experience* **27** (12): 1427-1456. DOI: 10.1002/1097-024X.

Bischof, C.H., Bucker, H.M., Lang, B. et al. 2002. Combining Source Transformation and Operator Overloading Techniques to Compute Derivatives for Matlab Programs. Paper presented at Second IEEE International Workshop on Source Code Analysis and Manipulation In Source Code Analysis and Manipulation, Montreal, Canada. DOI: 10.1109/SCAM.2002.1134106.

Brown, G.A., Davies, J.E., Collins, P.J. et al. 2005. Production Monitoring through Openhole Gravel-Pack Completions Using Permanently Installed Fiber-Optic Distributed Temperature Systems in the Bp-Operated Azeri Field in Azerbaijan. Paper SPE 95419 MS presented at the SPE Annual Technical Conference and Exhibition, Dallas, Texas, 9-12 October. DOI: 10.2118/95419-MS.

Bunge, H.P., Hagelberg, C., and Travis, B. 2003. Mantle Circulation Models with Variational Data Assimilation: Inferring Past Mantle Flow and Structure from Plate Motion Histories and Seismic Tomography. *Geophysical Journal International* **152** (2): 280-301. DOI: 10.1046/j.1365-246X.2003.01948.x.

Carrera, J. and Neuman, S.P. 1986. Estimation of Aquifer Parameters under Transient and Steady State Conditions: 1. Maximum Likelihood Method Incorporating Prior Information. *Water Resour. Res.* **22** (2): 199-210. DOI: 10.1029/WR022i002p00199.

Carrera, J. and Neuman, S.P. 1986. Estimation of Aquifer Parameters under Transient and Steady State Conditions: 2. Uniqueness, Stability, and Solution Algorithms. *Water Resour. Res.* **22** (2): 211-227. DOI: 10.1029/WR022i002p00211.

Carrera, J. and Neuman, S.P. 1986. Estimation of Aquifer Parameters under Transient and Steady State Conditions: 3. Application to Synthetic and Field Data. *Water Resour. Res.* **22** (2): 228-242. DOI: 10.1029/WR022i002p00228.

Duru, O. 2008. Modeling of Reservoir Temperature Transients, and Parameter Estimation Constrained to a Reservoir Temperature Model. MS thesis, Stanford University.

Feng, T., Mannseth, T., and Aanonsen, S.I. 2009. Randomized Maximum Likelihood with Permeability Samples Generated by a Predictor Corrector Technique. Paper SPE 118975 MS presented at the SPE Reservoir Simulation Symposium, The Woodlands, Texas, 2-4 February. DOI: 10.2118/118975-MS.

Finsterle, S. 1999. *Itough2 User's Guide*. Berkeley, CA: Lawrence Berkeley National Laboratory.

Fryer, V.I., Dong, S., Otsubo, Y. et al. 2005. Monitoring of Real-Time Temperature Profiles across Multizone Reservoirs During Production and Shut in Periods Using Permanent Fiber-Optic Distributed Temperature Systems. Paper SPE 92962 MS presented at the SPE Asia Pacific Oil and Gas Conference and Exhibition, Jakarta, Indonesia, 5-7 April. DOI: 10.2118/92962-MS.

Giering, R. and Kaminski, T. 1998. Recipes for Adjoint Code Construction. *ACM Transactions on Mathematical Software (TOMS)* **24** (4): 437-474. DOI: 10.1145/293686.293695.

Griewank, A., Juedes, D., and Utke, J. 1996. Algorithm 755: Adol-C: A Package for the Automatic Differentiation of Algorithms Written in C/C++. *ACM Transactions on Mathematical Software (TOMS)* **22** (2): 131-167. DOI: 10.1145/229473.229474.

Hansen, P.C. 1999. *The L-Curve and Its Use in the Numerical Treatment of Inverse Problems: IMM*. Copenhagen, Denmark: Technical University of Denmark, Department of Mathematical Modelling.

Hutchinson, D., Kuramshina, N., Sheydayev, A. et al. 2007. The New Interference Test: Reservoir Connectivity Information from Downhole Temperature Data. Paper SPE 11672 MS presented at International Petroleum Technology Conference, Dubai, U.A.E., 4-6 December. DOI: 10.2523/11672-MS.

Ikeda Naotsugu, S.C. 2002. Fiber-Optic Instantaneous Temperature Profile Log for Geothermal Reservoir Application. Paper SPWLA 2002-G presented at SPWLA 43rd Annual Logging Symposium, Houston, Texas.

Jafarpour, B., Goyal, V.K., Mclaughlin, D.B. et al. 2010. Compressed History Matching: Exploiting Transform-Domain Sparsity for Regularization of Nonlinear Dynamic Data Integration Problems. *Mathematical Geosciences* **42** (1): 1-27. DOI: 10.1007/s11004-009-9247-z.

Khaninezhad, M.R.M., Jafarpour, B., and Li, L. 2010. History Matching with Learned Sparse Dictionaries. Paper SPE 133654 MS presented at SPE Annual Technical Conference and Exhibition, Florence, Italy, 19-22 September. DOI: 10.2118/133654-MS.

Kiryukhin, A.V., Asaulova, N.P., and Finsterle, S. 2008. Inverse Modeling and Forecasting for the Exploitation of the Pauzhetsky Geothermal Field, Kamchatka, Russia. *Geothermics* **37** (5): 540-562.

Kosack, C., Vogt, C., Rath, V. et al. 2010. Stochastic Estimates of the Permeability Field of the Soultz-Sous-Forêts Geothermal Reservoir-Comparison of Bayesian Inversion, Mc Geostatistics, and Enkf Assimilation. EGU General Assembly, Vienna, Austria, 2-7 May.

Kragas, T.K., Williams, B.A., and Myers, G.A. 2001. The Optic Oil Field: Deployment and Application of Permanent in-Well Fiber Optic Sensing Systems for Production and Reservoir Monitoring. Paper SPE 71529 MS presented at the SPE Annual Technical Conference and Exhibition, New Orleans, Louisiana, 30 September-3 October. DOI: 10.2118/71529-MS.

Kühn, M. and Gessner, K. 2009. Coupled Process Models of Fluid Flow and Heat Transfer in Hydrothermal Systems in Three Dimensions. *Surveys in geophysics* **30** (3): 193-210. DOI: 10.1007/s10712-009-9060-8.

Li, L. and Jafarpour, B. 2010. Effective Solution of Nonlinear Subsurface Flow Inverse Problems in Sparse Bases. *Inverse Problems* **26**: 105016. DOI:10.1088/0266-5611/26/10/105016

Li, Z. and Zhu, D. 2010. Optimization of Production with Icv by Using Temperature Data Feedback in Horizontal Wells. Paper SPE 135156 MS presented at the SPE Annual Technical Conference and Exhibition, Florence, Italy, 19-22 September. DOI: 10.2118/135156-MS.

Likhachev, E. 2003. Dependence of Water Viscosity on Temperature and Pressure. *Technical Physics* **48** (4): 514-515. DOI: 10.1134/1.1568496

Marchuk, G.I. 1995. *Adjoint Equations and Analysis of Complex Systems*. Berlin, Germany: Springer.

Marchuk, G.I., Agoshkov, V.I., and Shutiaev, V. 1996. *Adjoint Equations and Perturbation Algorithms in Nonlinear Problems*. Florence, KY: CRC.

Moridis, G.J., Seol, Y., and Kneafsey, T.J. 2005. *Studies of Reaction Kinetics of Methane Hydrate Dissocation in Porous Media.* Berkeley, CA: Lawrence Berkeley National Laboratory.

Mukhopadhyay, S. 2009. Parameter Estimation from Flowing Fluid Temperature Logging Data in Unsaturated Fractured Rock Using Multiphase Inverse Modeling. *Water Resour. Res.* **45** (4): W04414. DOI: 10.1029/2008wr006869

Nath, D.K., Finley, D.B., and Kaura, J.D. 2006. Real-Time Fiber-Optic Distributed Temperature Sensing (DTS)-New Applications in the Oil Field. Paper SPE 103069 MS presented at the SPE Annual Technical Conference and Exhibition, San Antonio, Texas, 24-27 September. DOI: 10.2118/103069-MS.

Neuman, S. and Carrera, J. 1985. Maximum-Likelihood Adjoint-State Finite-Element Estimation of Groundwater Parameters under Steady-and Nonsteady-State Conditions. *Applied mathematics and computation* **17** (4): 405-432. DOI: 10.1016/0096-3003(85)90043-8.

Oliver, D.S., He, N., and Reynolds, A.C. 1996. Conditioning Permeability Fields to Pressure Data. Paper presented at 5th European Conference on the Mathematics of Oil Recovery, Mining University Leoben, Austria, September 3-6.

Oliver, D.S., Reynolds, A.C., and Liu, N. 2008. *Inverse Theory for Petroleum Reservoir Characterization and History Matching*. Combridge, UK: Cambridge Univ Press.

Peaceman, D.W. 1978. Interpretation of Well-Block Pressures in Numerical Reservoir Simulation. *Old SPE Journal* **18** (3): 183-194.

Pruess, K., Oldenburg, C., and Moridis, G. 1999. *Tough2 User's Guide*, Berkeley, CA: Lawrence Berkeley National Laboratory.

Rath, V., Wolf, A., and Bücker, H. 2006. Joint Three-Dimensional Inversion of Coupled Groundwater Flow and Heat Transfer Based on Automatic Differentiation: Sensitivity Calculation, Verification, and Synthetic Examples. *Geophysical Journal International* **167** (1): 453-466. DOI: 10.1111/j.1365-246X.2006.03074.x.

Remy, N., Boucher, A., and Wu, J. 2008. *Applied Geostatistics with Sgems: A User's Guide. Combridge,* UK: Cambridge Univ Press.

Somerton, W., El-Shaarani, A., and Mobarak, S. 1974. High Temperature Behavior of Rocks Associated with Geothermal Type Reservoirs. Paper SPE 4897 MS presented at SPE California Regional Meeting, San Francisco, California, 4-5 April. DOI: 10.2118/103069-MS.

Somerton, W., Keese, J., and Chu, S. 1973. Thermal Behavior of Unconsolidated Oil Sands. *Old SPE Journal* **14**(5): 513-521. DOI: 10.2118/4506-PA

Tarantola, A. and Valette, B. 1982. Generalized Nonlinear Inverse Problems Solved Using the Least Squares Criterion. *Rev. Geophys. Space Phys* **20** (2): 219-232. DOI:10.1029/RG020i002p00219

Tarantola, A. and Valette, B. 1982. Inverse Problems= Quest for Information. *J. geophys* **50** (3): 150-170.

Yoshioka, K., Zhu, D., Hill, A.D. et al. 2009. A New Inversion Method to Interpret Flow Profiles from Distributed Temperature and Pressure Measurements in Horizontal

Wells. *SPE Production & Operations* **24** (4): 510-521. DOI: 10.2118/109749-PA.

Zhang, F., Skjervheim, J.A., Reynolds, A.C. et al. 2003. Automatic History Matching in a Bayesian Framework, Example Applications. Paper SPE 84461 PA presented at the SPE Annual Technical Conference and Exhibition, Denver, Colorado, June. DOI: 10.2118/84461-PA.

VITA

Name:	Zhishuai Zhang
Address:	907 Richardson Building Department of Petroleum Engineering Texas A&M University College Station, TX 77843-3116
Email Address:	zhishuaizhang@gmail.com
Education:	B.S., Optical Information Science and Technology, Nankai University, 2010